AD-A166 034 USE OF THE SHADOW SPOT METHOD IN EVALUATING J FOR DUCTILE STEELS(U) BROWN UNIV PROVIDENCE RI DIV OF ENGINEERING A MARCHAND ET AL. FEB 86 ONR-0597/1 1/1

UNCLASSIFIED N00014-85-K-0597 F/G 20/11 NL

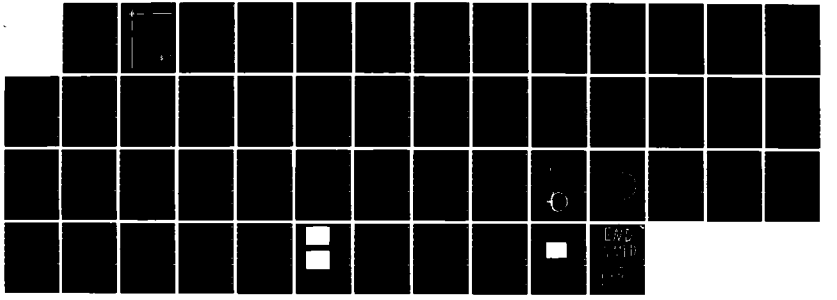

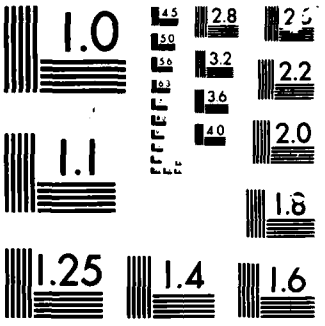

MICROCOPY CHART

Brown University
DIVISION OF ENGINEERING
PROVIDENCE, R.I. 02912

USE OF THE SHADOW SPOT METHOD IN EVALUATING J FOR DUCTILE STEELS

by

A. Marchand, L. B. Freund, C. C. Ma and J. Duffy
Division of Engineering, Brown University
Providence, R.I. 02912

Brown University
Division of Engineering
Providence, R.I. 02912

USE OF THE SHADOW SPOT METHOD IN EVALUATING J FOR DUCTILE STEELS

by

A. Marchand, L. B. Freund, C. C. Ma and J. Duffy
Division of Engineering, Brown University
Providence, R.I. 02912

Contract No. N00014-85-K-0597

Brown University Technical Report
ONR 0597/1
MRL E-160

February, 1986

"Use of the Shadow Spot Method in Evaluating J for Ductile Steels"

A. Marchand, L. B. Freund, C. C. Ma and J. Duffy

ABSTRACT

In fracture testing of ductile materials, it is important to characterize the crack tip mechanical fields in terms of measurable parameters, and the value of the J-integral is adopted here as a characterizing parameter. For a planar fracture specimen containing an edge crack and subjected to loading which results in mode I deformation, the lateral contraction of the specimen in the crack tip region is calculated in terms of J from the plane stress HRR asymptotic field of nonlinear-fracture mechanics. In a recent analysis, the caustic curve that would be generated by reflection of incident parallel light from points of the deformed specimen surface lying well within the crack tip plastic zone is determined for several values of the hardening exponent n [1]. A principal result of the analysis is a relationship between the observed diameter D of the shadow spot and the prevailing value of J. The purpose of the present article is to examine the validity of this expression. This is done through an experiment in which J is evaluated simultaneously by two *independent* experimental techniques. One of these techniques is the shadow spot method, and the other is a direct determination of J from the load and load point deflection data. Tests are performed with a modified double cantilever beam specimen with two different thicknesses. The materials are an oil-hardened tool steel and a 304 stainless steel. Results indicate agreement between the two inferred values of J provided that two size conditions dictated by the underlying analysis are met. One condition is that the initial curve must be deep enough into the plastic zone so that the HRR field can be expected to provide a reasonably accurate description of the prevailing strain distribution there. The second

condition is that the initial curve must be far enough from the crack tip so that conditions of plane stress are met along the initial curve. These conditions are assumed to be satisfied if the mean radius of the initial curve is less than one-third of the plastic zone size and greater than one-half the thickness of the plate specimen.

INTRODUCTION

Caustic curve patterns obtained by the shadow spot method have been used in the past to give direct optical measurement of the elastic stress intensity factor in nominally brittle material. An advantage of the optical shadow spot method is that it provides a direct measure of the intensity of the crack tip stress field. The method is based on the idea that the value of the stress intensity factor can be related to features of the optical field obtained by transmitting parallel light through the crack tip region of a transparent specimen or by reflecting light from the surface of an opaque specimen.

Most structural materials that contain cracks undergo substantial plastic deformation under rising load prior to onset of crack growh. Recently, the range of applicability of the shadow spot method was extended to the elastic-plastic power hardening materials [1]. It was noted that the value of Rice's J-integral can be viewed as a plastic strain intensity factor. Methods for measuring values of J for ductile fracture specimens are available but the methods are indirect, in the sense that values of J are inferred from other measured quantities, typically load-deflection data. The shadow spots obtained in the test should be formed by reflection of light rays from points well within the crack tip plastic zone where the one parameter plastic intensity singular field is dominant. The method of caustics provides a measurement which is customarily interpreted on the basis of plane stress theory. This approximate theory is believed to be valid only in cases in which the gradients of in-plane fields are small, and this criterion becomes increasingly difficult to meet as the observation point moves closer to the crack

tip. Hence, the region on the specimen where the information is sensed should be deep within the crack tip plastic zone where the plastic singular field can be expected to provide an accurate description of the local deformation field, but it should also be far enough from the crack tip so that the neglected three dimensional effects are not large enough to violate the two dimensional plane stress condition. A way to estimate this region on the specimen from the observed caustic curves on the screen is the main purpose of the next section.

II. THEORETICAL BACKGROUND

Consider a family of light rays parallel to the x_3 axis incident on the reflective surface $x_3 = f(x_1,x_2)$ of an opaque material. It is supposed that the specimen thickness is initially uniform, so that the function f represents the nonuniform lateral contraction due to deformation. Because of the nonuniform contraction at the crack tip, the reflected rays deviate from parallelism and, under suitable conditions, the family of rays possesses an envelope in the form of a three dimensional surface in space. This surface, which is called the caustic surface, is the locus of points of maximum density of reflected rays. Suppose a screen is placed parallel to the specimen at some distance z_0 in front of or behind the deformed specimen surface. If the screen intersects the three dimensional caustic surface in space, the image will be a completely dark area (the shadow spot) surrounded by a bright curve (the caustic curve). The locus of points on the specimen which map exactly into the caustic curve is called the initial curve. This property gives the initial curve its special importance. It will be shown subsequently that the size of the initial curve relative to the thickness of the specimen plays an important role in the analysis of caustics in the presence of crack tip plasticity. Experimentally, the plane of the screen will be the focal plane of a camera which is used to observe and record the caustic curve in the reflected light field. The caustic curves and

corresponding initial curves have been analyzed within the framework of plane stress theory.

If the plane of the specimen is the x_1, x_2-plane, then let the X_1, X_2-plane be the plane of the screen, where the screen's coordinate axes are obtained by translating the specimen's coordinate axes in the direction normal to the specimen, (see Fig. 1). It is now assumed for small deformation that $f << z_o$ and $f_{,i}f_{,i} << 1$. Under these conditions, the light ray which strikes the specimen at points x_i then intersects the screen at the point X_i given by

$$X_i = x_i - 2z_o \frac{\partial f}{\partial x_i}, \quad i = 1,2 \tag{2.1}$$

It was observed that applicability of the method does not hinge on a linear elastic response of the material in the crack tip region [1]. Instead, the key feature is that the deformed shape of the specimen surface in the crack tip region is known up to a scalar amplitude. In the case of elastic materials, this amplitude is the elastic stress intensity factor. Asymptotic elastic-plastic analyses of near crack tip fields for power hardening materials suggest that this situation may prevail for this case as well, and the value of the J-integral is adopted as the characterizing parameter. It was shown in [1] that for power hardening materials with hardening exponent n, the value of J is proportional to the diameter of the corresponding shadow spot raised to the power $(3n + 2)/n$.

For points deep within the crack tip plastic zone, the plastic field near the crack tip was analyzed by Hutchinson [2] and by Rice and Rosengren [3]. They limited consideration to the zone in the immediate neighborhood of a stationary crack tip where the plastic strains are large compared to the elastic strains, and to the case of a monotonically increasing applied load. They used a description of nonlinear elastic-plastic material response based on a power hardening relationship between rectangular components of plastic strain ϵ^p_{ij} and stress σ_{ij} of the form

$$\frac{\epsilon_{ij}^{p}}{\epsilon_0} = \frac{3}{2}\alpha \left(\frac{\sigma_e}{\sigma_0}\right)^{n-1} \frac{s_{ij}}{\sigma_0} \tag{2.2}$$

where

$$s_{ij} = \sigma_{ij} - \frac{1}{3}\sigma_{kk}\delta_{ij} ,$$

$$\sigma_e = \frac{3}{2} s_{ij}s_{ij}$$

and σ_0 is the tensile yield stress, ϵ_0 is the associated tensile yield strain, α is a material constant and σ_e is the effective stress. For a small strain formulation, the asymptotic strain distribution in the crack tip region is

$$\epsilon_{ij} = \epsilon_0 \left[\frac{J}{\sigma_0\epsilon_0 I_n r}\right]^{\frac{n}{n+1}} E_{ij}(n,\theta) . \tag{2.3}$$

The quantity I_n is a nondimensional parameter determined from the singularity analysis. Its value depends on n, and it ranges from about 5 for n = 1 to about 2.49 as n approaches infinity. Numerical values of the angular variation E_{ij} are available for many values of hardening exponent n from the work of Shih [4]. From the results in [1], the radius of the inital curve can be expressed as

$$r(n,\theta) = (HG)^{\frac{n+1}{3n+2}} \tag{2.4}$$

where

$$H = \frac{\alpha + \sqrt{\alpha^2 + 4\beta}}{2}$$

$$\alpha(n,\theta) = \left(\frac{n}{n+1}\right)^2 \psi + \psi''$$

$$\beta(n,\theta) = \frac{2n+1}{n+1}\left[\left(\frac{n}{n+1}\right)^2 \psi^2 - \frac{n}{n+1}\psi\psi'' + \frac{2n+1}{n+1}(\psi')^2\right]$$

$$G = B\,\epsilon_0 z_0 \left[\frac{J}{\epsilon_0 \sigma_0 I_n}\right]^{\frac{n}{n+1}}$$

$$\psi(n,\theta) = E_{rr}(n,\theta) + E_{\theta\theta}(n,\theta)$$

The prime denotes the derivative with respect to θ. Equation (2.4) gives the initial curve on the specimen surface for a given intensity of local deformation field. The size of the initial curve depends on the specimen thickness B, the distance z_0 and the strength of the plastic strain singularity J. The numerically determined initial curve for n = 2, 3, 5, 9, 25 is shown in Fig. 2. It indicates that the shape of the initial curve depends strongly on the strain hardening exponent n. For small n, the initial curve is almost circular, and it elongates in the y direction as n increases.

The points on the initial curve as expressed in (2.4) will map to the corresponding caustic curve on the screen according to (2.1). Adopting the maximum transverse diameter, denoted D, as the characteristic dimension, the intensity of the strain singularity can be expressed as [1]

$$J = S_n \epsilon_0 \sigma_0 \alpha \left[\frac{1}{\alpha \epsilon_0 z_0 B}\right]^{\frac{n+1}{n}} D^{\frac{3n+2}{n}} \qquad (2.5)$$

where S_n is a numerical constant depending on n and expressed as:

$$S_n = -\ 0.0712 + 0.54e^{-1/n} - 1.1375e^{-2/n} + 1.2936e^{-3/n} - 0.556e^{-4/n}$$

Equation (2.5) provides a simple relationship between the size of an observed caustic and the strength of the plastic strain singularity near the tip of a crack in an elastic-plastic power law hardening material under plane stress conditions.

For the linear elastic case n = 1, the initial curve in (2.4) reduces to a circle with the radius

$$r_e = \left[\frac{3z_0 B\nu K}{2\sqrt{2\pi}E}\right]^{2/5} \tag{2.6}$$

where E is the elastic modulus and ν is Poisson's ratio. The relationship between the size of an observed caustic curve and the elastic stress intensity factor K is

$$K = \frac{ED^{5/2}}{10.71 z_0 B\nu}$$

in this case. Using the relation $J = K^2/E$ for the elastic case, J can be written as

$$J = \frac{0.0087 E D^5}{B^2 \nu^2 z_0^2} \tag{2.7}$$

To gain further insight into the optical phenomenon, the reflected optical fields were simulated numerically and displayed by means of a computer plotter. A closely spaced rectangular array of parallel light rays was assumed to be incident on the deformed specimen surface. The pattern of reflected rays that would be observed by a camera focussed on a suitable plane behind the specimen is shown in Fig. 3 for n = 1 and n = 3. The central parts of these simulated reflected fields contain no rays, and these parts are the shadow spots. The reflected rays are most dense on the perimeters of the shadow spots, and these perimeters are the caustic curves. Another way to obtain the same caustic curves is to directly map the initial curves (2.4) according to the formula (2.1). The numerically determined caustic curve for n = 2, 3, 5, 7, 9, 13, 25, and 100 is shown in Fig. 4.

A caustic curve observed on the screen corresponds to a mapping of the initial curve located on the specimen. Since the stress field at the crack tip is interpreted in terms of the stress intensity factor, the analysis is appropriate only in a specific region around the crack tip. Thus the reliability of the method of caustics depends on the location of the initial curve which can be varied by changing the focussed distance z_0 in

the optical set up (see Fig. 9). Increasing or decreasing z_o will cause the initial curve to move away from or toward the crack tip. If the plastic intensity factor J is the parameter to be determined by means of the shadow spot method applied to ductile material, then the initial curve should be located within the HRR dominated zone; see Fig. 5. If the caustic method is applied to brittle materials, the initial curve should be located in the elastic field so as to evaluate the elastic stress intensity factor K at the crack tip; see Fig. 5. A proper choice of z_o will place the initial curve either within the region of dominance of the HRR singularity, or within the stress intensity factor controlled region.

From equations (2.4) and (2.5), the relationship between the observed maximum diameter D and the corresponding initial curve radius r is found to depend only on the hardening exponent n and the angular position θ,

$$D = r \left[\frac{I_n}{S_n}\right]^{\frac{n}{3n+2}} H^{\frac{1-n}{3n+2}} \tag{2.8}$$

Numerical analysis indicates that the shape of the initial curve depends strongly on the strain hardening exponent, Fig. 2. The initial curve "radius" r, defined as the distance from the crack tip to the initial curve, is a function of n and the angular position θ. Figure 6 defines three essential values of the distance $r(\theta,n)$ used to characterize the size and shape of the initial curve: $r_{ox} = r(0,n)$ = the distance in the x-direction, r_{oy} = the maximum distance in the y-direction, and $r_o = r(\theta_{max}(n), n)$ = the distance to the point of the initial curve which maps on the maximum transverse diameter of the caustic.

From the numerical computation, the value of θ_{max} is calculated for some n. For n = 1, $\theta_{max} = 72^\circ$, and it decreases to 68°, 65°, 62.5°, 61°, 59.5°, 58.5°, 57.5°, 56.5°, 56° for n = 2, 3, 4, 5, 7, 9, 13, 25 and 100.

The numerical analysis relates the maximum diameter D of the caustic to each of these three parameters through

$$D = R_o(n)r_{ox} = R_i(n)r_{oy} = R_c(n)r_o \tag{2.9}$$

where

$$R_o(n) = 3.516 - 1.552e^{-1/n} + 2.954e^{-2/n} - 4.33e^{-3/n} + 2.21e^{-4/n}$$

$$R_i(n) = -0.135 + 23.44e^{-1/n} - 58.91e^{-2/n} + 62.45e^{-3/n} - 24.81e^{-4/n}$$

$$R_c(n) = 4.70 - 9.62e^{-1/n} + 22.7e^{-2/n} - 24.7e^{-3/n} + 9.45e^{-4/n}$$

Figure 7 gives the variation of the functions $R_o(n)$, $R_i(n)$, $R_c(n)$ with the strain hardening exponent n. They appear to be strongly dependent on n. For the linear elastic case (n = 1), the initial curve is circular and the radius r is constant. Then the above functions are simply

$$R_o(1) = R_i(1) = R_c(1) = 3.17 \tag{2.10}$$

Hence from the results shown in Fig. 2 and Fig. 7, enough information is available about the initial curve to estimate its shape and its size, and to locate its distance from the crack tip, by measuring the diameter D of the corresponding caustic curve observed on the screen. These results provide important information which will be used in the next section to interpret the experimental work.

III - EXPERIMENTS

1. J-Integral Reference Value

The aim of this research is to evaluate the J-integral based on data derived from the caustics experiment and compare the resulting values of J with reference values based on the load-displacement record obtained in the same test. In general, the J-integral can be interpreted as the rate of energy release with respect to crack length for nonlinear elastic materials. For this reason, some studies have been

carried out to express J as a function only of load and displacement so as to apply it for any crack length. Rice et al. [5] developed a method for deeply cracked 3-point bend and compact specimens in which the value of J is determined as a function of load point displacement δ through

$$J(P, \delta) = \frac{2A(P, \delta)}{B \times b} \qquad (3.1)$$

where $A(P,\delta)$ is the area under the load-displacement curve at a given displacement δ, b is the length of the uncracked ligament and B is the specimen thickness. However, based on the results of a series of experiments, Landes et al. [6] showed that this expression underestimates the J value as determined by the energy rate interpretation.

Merkle and Corten [7] developed a theory, also based on compliance analysis, for a compact tension specimen (CTS) with a fully yielded ligament. Their solution holds for the linear elastic case when $a/W \geq 0.5$, where a is the crack length and W the specimen length, and for the rigid plastic case for all geometries. By assuming that the complementary energy is much smaller than the total energy, a simplification of their result was made by Landes, et al. [6] that provides the following expression:

$$J(P, \delta) = \eta_r \frac{A(P, \delta)}{B \times b} \qquad (3.2)$$

where $\eta_r = \dfrac{2(1 + \zeta)}{1 + \zeta^2}$

$$\zeta = 2[(a/b)^2 + (a/b) + 1/2]^{1/2} - 2(a/b + 1/2)$$

According to Landes et al. [6], this expression, when applied to the CTS, provides the best approximation for J from small scale yielding conditions to fully plastic conditions for $a/W \geq 0.5$; it does not depend on the material behavior (elastic or plastic) at the crack tip. For these reasons, the expression for J provided by

Equation (3.2) is taken as the reference value in the present paper.

2. Loading Fixture - Specimen Design and Preparation

It is common, in fracture experiments using the caustics method, to employ a double cantilever beam (DCB) specimen. For the present experiments, however, the shape of the specimen had to be modified. As previously seen, we must record the load P and the displacement δ during the test so as to evaluate the reference value of J. Wedge-loading of the customary DCB specimen cannot be employed, however, since the frictional component of the applied force would make it difficult to arrive at an accurate value of the separating force. As a result, the specimen was modified so a short hydraulic cylinder jack of 25.4 mm diameter could be inserted between the beams of the specimen (see Figure 8). This jack was chosen to have a maximum displacement large enough to deform fully and plastically a wide range of materials. With the jack in place, the load is applied and recorded by means of a pressure transducer. The relative displacement of the two load points is measured by a differential transformer and recorded against the load on an x-y plotter.

Some preliminary tests on AISI 1020 hot-rolled steel specimens allowed us to establish a specimen size suitable for our purposes, a comparison between the two experimental values of J being possible only when the plastic zone is confined to the crack tip region. However, in these preliminary tests, we noticed that when the displacement δ (or load P) reached a critical value δ_c (or P_c), some plastic deformation appeared at the outer edges of the beams making it impossible to obtain an accurate value of J by the load-displacement method. In order to eliminate the plastic deformation at the outer edges of the beams a further modification was effected in the shape of the specimen, in which the beams were made thicker than the central portion of the specimen. This was done by starting with a thick specimen, 12.7 mm, and thinning it in the region of the crack by milling a groove

5 cm. wide along the crack path on both faces of the specimen. Furthermore, in order to increase δ_c, and also measure more precisely the displacement δ, we used a reasonably long crack length a, about 18.5 cm, giving the specimen a length W of 27.9 cm (a/W = 0.66) and a width of 15.2 cm. In addition, by thickening the two beams, the value of δ_c was also increased.

In these experiments, considerable attention was given to the preparation of the specimens. The starter crack was first cut using a saw and then, in order to achieve a "sharp" crack tip, the crack was extended another 8 mm by employing an EDM spark cutter. The resultant crack tip was given a width of either 0.5 mm or 0.27 mm by using electrodes of two different thicknesses.

Since the specimen material is opaque, the caustic was formed by reflection of light from the specimen's surface. For this purpose the surface is kept flat and polished to a mirror finish. This was achieved by grinding and then polishing the surface, as described in Reference [1].

Lastly, the significance of the specimen thickness was also examined in this study. For each material studied, two thicknesses were tested: 6.35 mm and 12.7 mm.

3. Some Relevant Remarks

For an accurate determination of the value of J through the load-deflection method, it is necessary that all plastic deformation in the specimen be confined to the neighborhood of the crack tip. For our specimen shape, since some plastic zone eventually will appear at the edges when the load is increased sufficiently, the plastic zone at the crack tip may not extend all the way to the bottom of the specimen. However, the plastic zone size surrounding the crack tip is large enough to make us confident that the material's response is one of large scale yielding in the neighborhood of the crack tip. A necessary condition to produce fully plastic

behavior in a compact tension specimen is that the specimen length must be about 1.2 times the specimen length W [8]. In our case, this ratio is about 0.55, and this explains why the load is limited to a critical upper value P_c when plastic deformation appears at the edges. However the range of load values suitable to our comparative study is quite large.

A lower bound for the load P_L is defined by two related criteria: the plane stress condition and the size of the plastic zone in which the HRR field dominates. A recent analysis carried out by Yang and Freund [9] for an elastic plate shows that plane stress prevails at distances r from the crack tip up to one-half to three-fourths of the plate thickness B, depending on the value of Poisson's ratio. Some experiments performed by Rosakis and Ravichandar [10] on elastic materials using the method of caustics, analyzed consistent with plane stress conditions, confirm this solution. Their results show that a plane stress field is approached at r/B = 0.5 for which the experimental elastic stress intensity factor K_{exp} is found to be 90% of the theoretical value K_{th}. On the other hand, for ductile materials, the extent of the plane stress field remains unknown at the present time.

The second criterion has to do with the plastic zone size, which must be large enough to include the HRR field under plane stress conditions. Some numerical analyses, for small scale yielding and plane strain conditions, have shown that the HRR field dominates at a distance R ahead of the crack tip of approximately

$$R \sim \left[\frac{1}{5} \text{ to } \frac{1}{4}\right] R_{px} \qquad (3.3)$$

where R_{px} is the distance to the boundary of the plastic zone ahead of the crack tip. For the bend configuration and the compact tension specimen under fully plastic and plane strain conditions, numerical studies [11] indicate that

$$R \sim 0.07b \qquad (3.4)$$

where b is the length of the uncracked ligament, i.e. W-a.

In their analysis of applicability of caustics experiments to ductile materials, Rosakis et al. [1] tried to define a criterion for satisfying the condition of incompressibility of material response. For plane stress conditions, they used the HRR asymptotic strain distribution ahead of the crack tip along the x-axis for a perfectly-plastic material to derive

$$\epsilon_{22}/\epsilon_0 = 0.9\ (R_{px}/r) \tag{3.5}$$

where ϵ_0 is the yield strain. By assuming that the ratio ϵ_{22}/ϵ_0 must be greater than 2 or 3, Rosakis et al. [1] showed that the ratio of the distance R to the plastic zone size R_{px} along the x-axis must be

$$\frac{R}{R_{px}} < \frac{1}{2} \text{ or } \frac{1}{3}\ . \tag{3.6}$$

The region of dominance of the HRR singularity fields in plane stress conditions and large scale yielding behavior has not been examined yet. Using plane strain results as a guide, it can be expected that the numerical analysis in plane stress will show that the size of this region depends strongly on the specimen configuration and on the strain hardening behavior of the material. Section 7 of this report shows that the method of caustics is an experimental method well suited to this specific problem.

4. Optical Set-Up

Figure 9 shows the optical set-up adopted for our static caustics experiments. A beam of parallel light rays impinges upon the specimen at an angle α and is reflected towards the screen S_c, passing through a system of either one or two lenses, depending on the total necessary magnification to measure precisely the caustic diameter D. The camera is placed behind the screen and focussed on it. A helium-neon laser light of 25 milliwatts maximum output was used to improve the clarity of the caustic. This arrangement is very precise in the determination of z_0

and D, and allows for a large range of values of z_0, i.e. a large range for the initial curve radius r_0 ($0.25 \leq r_0/B \leq 2.5$ where B is the specimen thickness and the given values come from a numerical analysis in the HRR singularity field).

In using this arrangement it is important to make the angle α as small as possible. Separate tests were conducted to see if the value of α influenced the observed width of the caustic. These tests were performed by using a half-silvered mirror in order to reduce α to zero, i.e. in order to direct the light beams normally onto the specimen's surface. Although this technique does not provide sufficient light for conventional testing it serves as a valuable check; and it indicated that a value of α less than 10° made no observable change in the width of the caustic.

For the optical set-up shown in Figure 9, the distance z_0 behind the specimen, on which the camera is focussed, is evaluated from the equation for a thin lens,

$$\frac{1}{p + z_0} + \frac{1}{q} = \frac{1}{f_1} \tag{3.7a}$$

where p is the distance from the specimen to the lens L_1, q is the distance from the lens L_1 to the screen S_c and f_1 is the focal length of the lens L_1. The total magnification λ is given by

$$\lambda = \left[\frac{q}{f_1} - 1\right] \tag{3.7b}$$

The focal length f_1 and the distance p being established, different distances z_0 are obtained by moving the screen S_c perpendicularly to the light beam, i.e. varying the image distance q.

Once the distance z_0 is established, the corresponding maximum diameter D of the caustic is evaluated by means of the relation $D = \Delta/\lambda$, where Δ is the direct measure of the diameter on the screen S_c. The total magnification λ is determined from a scale mounted on an unstrained portion of the surface of the specimen [12]. For ductile materials, because of the large plastic zone, the scale has to be mounted

in a zone quite far from the crack tip and therefore generally not illuminated by the laser. Quite a precise value of λ is achieved by using the above method, equation (3.7).

From equation (3.7), it appears that a large distance z_0 is obtained by decreasing the distance q. When q approaches the focal length f_1, Figure 9 shows that the beam size becomes smaller. A second lens then is inserted into the optical set-up between the lens L_1 and the screen S_c. This lens is used to enlarge the image and thus allows for a more precise measurement of caustic diameter Δ. The size of the initial curve r_0 depends upon the distance z_0, a larger z_0 giving a greater r_0. The initial curve can thus be located either outside or inside the plastic zone. Therefore the shape and the diameter D of the caustic change with the distance z_0. For instance, when the initial curve is inside the elastic field (large radius r_0), the caustic looks like a circle, while for an initial curve inside the HRR field (inside the plastic zone), the shape of the caustic depends on the strain hardening exponent n.

It is obvious that the amount by which the specimen thickness decreases in the neighborhood of the crack tip, creating the optical effect on which the existence of the caustic depends, varies with the applied load P. Thus both the distance z_0 and the load P affect the caustic size. An increase of P at fixed z_0, or of z_0 at fixed P, leads to enlargement of the diameter D on the screen S_c. This means that, in both cases, the radius r of the initial curve, which is the locus of points having the same deflection u_3, also increases. The main difference is that in the first case u_3 remains constant, while in the second it decreases.

5. Materials

The chemical compositions of the two steels used in the present experiments is presented in Table 1. Figure 10 gives the quasi-static tensile stress-strain curve along with mechanical parameters derived from these curves for these steels. In this

table, σ_0 represents the experimentally determined yield stress at an offset strain of $\epsilon_0 = 0.20\%$. The parameters α and n, the latter representing the strain hardening exponent, are chosen to match the Ramberg-Osgood [13] stress-strain relation

$$\epsilon/\epsilon_0 = \sigma/\sigma_0 + \alpha(\sigma/\sigma_0)^n \tag{3.8}$$

since this is the equation generally adopted in defining HRR singularity fields. The evaluation of the parameters for the 304 stainless steel was relatively straight-forward since the experimental points form a smooth curve (Figure 10). In the case of the tool steel some material instabilities are visible at initial yield and only the plastic portion of the curve following these instabilities was used in the modelling.

Some preliminary fracture tests were also performed on an AISI 1020 hot-rolled steel. In spite of extra care taken in polishing the surfaces of these specimens, the shadow spot was very poorly defined. It is believed that this blurring of the shadow spot is due to Luder's bands emanating from the plastic zone. Indeed, as loading continues, the elastic-plastic boundary on the specimen becomes visibly more and more ragged until plastic zones are seen to shoot out. This non-uniform plastic strain distribution in the metal produces a caustic with a blurred boundary that is, therefore, difficult to interpret. Accordingly, no results are presented for this steel.

6. Experimental Procedure

With the instrumented specimen and the optics in place, as described in Sections 2 and 4, a load P is applied and maintained fixed. The corresponding area $A(P,\delta)$ under the load-displacement curve is then calculated, and by invoking Equation (3.2) it now becomes possible to obtain a reference value for $J(P,\delta)$ appropriate to the particular value of P. Next, the caustic diameter D is measured on the screen S_c for several values of z_0. For a given load P, the curve $D(z_0)$ is called the caustic envelope. The value of J, noted J_s, is calculated using either

Equation (2.5) or (2.7) depending upon the extent of plastic strain at the crack tip. All these calculations are performed during the course of the experiment in order to find the exact positions of the screen S_c for which J_s, evaluated either by the elastic or the plastic equation, is equal to J(P,6). By this process the initial curve is located either inside the K field or inside the HRR field (Figure 5). Some representative photographs were taken in order to show the different shapes of caustics corresponding to different values of the ratio r_o/B, Figures 17 and 24.

For purposes of analysis, it is necessary to compare the plastic zone size surrounding the crack tip with the size of the initial curve. In the case of the 1020 steel or the tool steel, this size is macroscopically well defined by slip-lines, and can be measured directly. But the 304 stainless steel does not show slip lines. At the present time, no numerical analysis is available that provides an estimate of the plastic zone size in large scale yielding and for plane stress conditions. For the 304 stainless steel we observe that the surface of the specimen gradually loses its reflectivity when plastic deformations are imposed. The size of this region, like the plastic zone size, increases with load. Furthermore, as z_o is decreased, the initial curve shrinks toward the crack tip, where larger deformations are present; the corresponding caustic becomes blurred and the diameter Δ ceases to be measurable.

7. Results

The results of two experiments are presented for each of the two steels tested. The experiments were performed with specimens of two thicknesses (6.35 mm and 12.7 mm) and two widths for the crack tip (0.27 mm and 0.50 mm). The crack length a was established such that the ratio a/W was equal to 0.66 for three specimens and 0.696 for one specimen. The experiments were stopped before any crack growth. The results of these experiments are presented as follows:

1. Evaluation of J Based on Results of the Load-Displacement Experiments

For each specimen, with an initial specific value of the ratio a/W, the load

P divided by the specimen thickness is plotted against the load-line displacement δ, Figures 11 and 18. Figure 11 represents an average curve of tests with three specimens of the tool steel. After calculating the area $A(P,\delta)$ under each curve at various displacement values δ, the reference values $J(P,\delta)$ are calculated as functions of δ used in Equation (3.2), Figures 12 and 19.

2. Evaluation of J Based on Results of the Caustics Experiments

As described previously, a typical test consists in loading the specimen to a number of values of the load P. With P fixed, the diameter of the caustic D is measured for various settings of z_o. These values of D are then plotted as functions of z_o. Typical results are shown in Figures 13 and 15 for the tool steel and Figures 20 and 22 for the stainless steel.

For three of these specimens, the crack was cut with a width of 0.50 mm and with a square crack tip, Figures 13, 20 and 22. Under these conditions a power law function of the form

$$D = \beta z_o^{\gamma} \tag{3.9}$$

fits the results quite satisfactorily, as may be seen by the solid lines drawn in the figures.

For each fixed value of the load P and for each point (D,z_o) we evaluate J_s and compare it to the reference value $J(P,\delta)$. In order to apply the elastic expression for J, Equation (2.7), and then compare it to the reference value $J(P,\delta)$, measurements were taken at a very low load for each test, i.e. within the limits of small scale yielding. Under these conditions, the caustics appeared circular but very small and blurred so that elastic measurements of J were not valid because the condition $r_o/B \geq 0.5$ was not met. As the plastic zone increases with load, the K field will be erased and the plastic expression for J will be used. Thus the results only deal with the validity of the expression for J derived for a power law hardening material.

In Figures 14, 21, 23, the values of $J_s/J(P,\delta)$ versus r_o/B are plotted for different loads. The arrows indicate the restrictive domains of r_o/B in which $0.9 \leq J_s/J(P,\delta) \leq 1.1$. They represent regions ahead of the crack tip where the HRR singularity fields provide a good approximation. The effect of a sharper crack tip (0.27 mm wide) becomes clear in Figure 16, where J_s is plotted against r_o/B so as to distinguish each curve corresponding to different values of $J(P,\delta)$.

The size of the plastic zone has been defined and measured in two directions (Figure 4):

R_{px} = the maximum extent of the zone ahead of the crack tip in the x-direction,

R_{py} = the maximum extent of the zone in the y-direction.

For the tool steel, measurements were taken directly from the macroscopically observable plastic zone. Tables 2 and 3 give for different values of $J(P,\delta)$ the minimum and the maximum values of r_o/B for which $J_s/J(P,\delta)$ lies in the range 0.9 to 1.1. Table 2 gives a comparison of the plastic zone size, defined by R_{px} and R_{py}, with the initial curve radii r_{ox} and r_{oy} corresponding to the preceding values of r_o/B.

8. Discussion

Figures 14, 16, 21 and 23 provide values of the ratio $J_s/J(P,\delta)$ as functions of r_o/B for each of the two steels. Each curve in these figures represents one value of the applied load and hence gives a range of validity for J_s as a function of r_o/B. This range of validity of r_o/B is a restricted domain of the initial curve radius r_o in which the HRR fields provides a good approximation to the value of J. In order to locate this restricted region, the values of the initial curve radius are compared with the specimen thickness B and with the extent of the plastic zone. For each specimen tested, the value of J_s approaches the reference value $J(P,\delta)$ when the ratio r_o/B is greater than 0.5. This means that a plane stress field is reached only at

a distance r ahead of the crack tip greater than half the thickness. Hence, the dominance of plane stress conditions, which are known to hold in the elastic case, appear to hold as well for the ductile deformation in specimens of the steels tested.

For values of r_0/B greater than 0.5, it appears that the shape of the curve $J_S/J(p,\delta)$ versus r_0/B can be affected strongly by the sharpness of the crack tip. The role of crack tip width and sharpness were investigated for the tool steel with results as shown in Figures 14 and 16. For the 304 stainless steel, specimens were tested with a blunt crack tip, Figures 21 and 23. For a blunt crack tip, one with a width of 0.50 mm, Figures 14, 21, 23, the ratio $J_S/J(p,\delta)$ continues to increase indefinitely as r_0/B is increased (up to the highest value tested, $r_0/B = 2.5$). Hence the J_S expression overestimates the value of J as compared to the load point-displacement value. On the other hand, with a sharper crack tip, 0.27 mm wide, Figure 16, for each value of the applied load, a shelf appears such that $0.9 \leq J_S/J(P,\delta) \leq 1.1$ after which the ratio $J_S/J(P,\delta)$ decreases very rapidly, the plastic expression for J evaluated in the HRR field underestimates the value of $J(P,\delta)$.

Whether the crack tip is narrow or wide, as the load increases the plastic zone becomes more extensive. Simultaneously the zone of dominance of the HRR field increases in diameter. However, the width of the HRR field depends on the width of the crack tip. For a wide crack tip, the width of the HRR field remains constant as the load and its diameter increase. For a sharp crack tip, the width of the HRR field increases as its diameter and the load increase. This is implied by the results presented in Figures 14 and 16 and Table 2 for the tool steel: the region of validity broadens by a factor of about two between the lower and upper values of $J(P,\delta)$, shown by curves 1 and 3 in Figure 16, and whose values are indicated.

Direct measurements of the size of the plastic zone on the specimen's surface show that the relative location of the HRR field with respect to the plastic zone is independent of load, but depends on the specimen thickness and the shape of the

crack tip. The following estimates give the region of dominance of the HRR singularity field in plane stress for large scale yielding conditions, for n = 4.26 as in the tool steel. As may be seen in Table 2, the condition prescribed by Equation (3.6) is satisfied for both a sharp and a blunt crack tip. However, the measurement imposed by Equation (3.3) is satisfied for a sharp crack tip, but is not satisfied for the blunt crack tip. Values of r_{ox}/R_{px} in the range 0.32 to 0.35 exceed the values presented in Equation (3.3).

The ratio ϵ_e/ϵ_o, where ϵ_e is the effective deformation given by the following equation $\epsilon_e^2 = 2/3\ \epsilon_{ij}\epsilon_{ij}$, where ϵ_{ij} is the asymptotic strain distribution in the crack tip region given by equation (2.3), has been evaluated for the minimum and the maximum values of r_o/B in the HRR field and different values of J(P,δ). For the materials and the thicknesses tested, it appears that the minimum value of ϵ_e/ϵ_o is about 1. The ratio ϵ_e/ϵ_o equals unity only at the lowest value of load P for which plane stress conditions are met and for which the ratio r_{ox}/R_{px} satisfies the previous estimate. This ratio increases with load; we find the maximum value $\epsilon_e/\epsilon_o \simeq 3.5$ for B = 6.40 mm and $\epsilon_e/\epsilon_o \simeq 9$ for B = 012 mm. The fact that ϵ_e/ϵ_o is equal to or greater than unity confirms the fact that the initial curve always lies well within the plastic zone.

Figures 17a and 17b show two photographs of caustics obtained for the tool steel with specimen No. 4 tested with a sharp crack tip. The photographs were taken at the same load but for two values of the ratio r_o/B corresponding to two values of the distance z_o. In both photographs, slip lines can be made out in the mottled region surrounding the shadow spot. Calculations indicate that the initial curves lie well within the plastic zone. The caustic diameter is measured, as shown, as the maximum width of the shadow spot in a direction perpendicular to the crack tip. The shadow spot and hence its width appear better defined in Figure 17(a) than in (b). The blur in Figure 17(b) is due probably to the presence of the slip lines in the neighborhood of the crack tip and the fact that the shadow spot lies well inside this blurred region. The photograph in Figure 17(a) is taken for a ratio $r_o/B = 0.272$, giving $J_S/J(P,\delta) = 0.221$,

which indicates that plane stress conditions are not satisfied. In this case, the ratio r_{ox}/R_{px} is equal to about 1/12 and the distance r_{ox} does not satisfy the conditions specified by Equation (3.3). The slip lines emanating from the crack tip indicate that the initial curve is very close to the process zone where intense deformations are induced. For Figure 17 (b) the ratio $r_o/B = 0.533$, giving $J_s/J(P,\delta) = 1.06$, which indicates that the initial curve is inside the elastic-plastic HRR field and that plane stress conditions are met. In this instance, the ratio r_{ox}/R_{px} is equal to 1/4.63 which falls within the bounds imposed for the applicability of Equation (3.3).

The caustics obtained with the 304 stainless steel with specimen number 2, Figure 24, appear brighter than those obtained with the tool steel. This is because the stainless steel does not show slip lines, even at higher loads. In spite of that, as the load increases and the plastic zone grows, this material loses more reflectivity than the tool steel, particularly in the region surrrounding the crack tip where plastic deformation is more intense. As a result, the caustic diameter D ceases to be measurable. This phenomenon becomes a hindrance in the experiment when higher loads are reached. In the present tests, the caustic in the 304 stainless steel becomes blurred for a ratio $r_o/B = 0.70$ of the corresponding initial curve, when the load per unit thickness attains a value of 1.08 kN/mm. This introduces another load limitation since r_o/B in the present tests cannot be less than 0.7, so that the initial curve cannot be located in the HRR dominated zone. However, if the load per unit thickness is less than 1.08 kN/mm, Figure 24 shows a caustic for a 304 stainless steel specimen, taken for $r_o/B = 0.665$ giving $J_s/J(P,\delta) = 0.976$: the corresponding initial curve lies inside HRR field and plane stress conditions are satisfied. While a wider specimen might be useful to concentrate all plastic deformation at the crack tip, very wide specimens of the 304 stainless steel cannot be carrried to high loads.

9. Conclusions

The object of the experiments described was to determine the validity of the expression for the plastic strain concentration factor J, as derived by Freund and co-workers, for ductile materials and applicable to caustics experiments. According to the analysis, this expression is valid as long as the initial curve is located within the region of the plastic zone where the plane stress HRR singularity field dominates, and not valid elsewhere. An experiment was conducted in order to evaluate J simultaneously by the caustics method and by a load-displacement analysis. The latter analysis gives a reference value of J. The results may be summarized as follows:

1. A plane stress field is reached at a distance r ahead of the crack tip greater than half the thickness B.
2. The HRR field, where direct plastic measurements of J are possible, is a zone whose limits increase with load. It is located at a distance R from the crack tip such that, for n = 4.26, and for a sharp crack tip,

$$R/R_{px} = \left(\frac{1}{4} \text{ to } \frac{1}{5}\right)$$

where R_{px} is the extent of plastic zone ahead of the crack tip. The ratio R/R_{px} is independent of the load. The results of the experiment show that the optical method of caustics provides a powerful experimental tool for the characterization of this region under plane stress conditions, through the extent of the plastic zone.

Acknowledgements

The research support of the Office of Naval Research, Structural Mechanics Program, Grant N00014-85-K-0597, and the NSF Materials Research Laboratory at Brown University is gratefully acknowledged. Thanks also are due to Professor C. F. Shih for helpful discussions and suggestions.

REFERENCES

1. Rosakis, A. J., Ma, C. C. and Freund, L. B., "Analysis of the Optical Shadow Spot Method for a Tensile Crack in a Power-Law Hardening Material," *ASME Journal of Applied Mechanics*, Vol. 50, 1983, pp. 777-782.

2. Hutchinson, J.W., "Singular Behavior at the End of a Tensile Crack," *Journal of the Mechanics and Physics of Solids*, Vol. 16, 1968, pp. 13-31.

3. Rice, J.R., and Rosengren, G.F., "Plane Strain Deformation Near a Crack Tip in Power Law Hardening Materials," *Journal of the Mechanics and Physics of Solids*, Vol. 16, 1968 p. 1-12.

4. Shih, C.F., "Elastic-Plastic Analysis of Combined Mode Crack Problems," Ph.D. Thesis, 1973, Harvard University.

5. Rice, J. R., Paris, P. C. and Merkle, J. G., "Some Further Results of J-Integral Analysis and Estimates," in *Progress in Flaw Growth and Fracture Toughness Testing*, ASTM STP 536, ASTM 1973, pp. 231-245.

6. Landes, J. D., Walker, H., and Clarke, G. A., "Evaluation of Estimation Procedures Used in J-Integral Testing," in *Elastic-Plastic Fracture*, ASTM STP 668, ASTM 1979, pp. 266-287.

7. Merkle, J. G., Corten, H. T., "A J-Integral Analysis for the Compact Specimen, Considering Axial Force as Well as Bending Effects," ASME Paper No. 74-PVP-33, American Society of Mechanical Engineers, 1974.

8. Shih, C. F., German, M. D., Kumar, V., "Estimation Technique for the Prediction of Elastic-Plastic Fracture of Structural Components of Nuclear Systems," 2nd and 3rd Semi-Annual Report to EPRI, General Electric Company, Schenectady, New York, January 1980.

9. Yang, W. and Freund, L. B., "Transverse Shear Effects for Through-Cracks in an Elastic Plate," Brouwn University Report (1984).

10. Rosakis, A. J. and Ravichandar, K., "On Crack Tip Stress State: An Experimental Evaluation of Three Dimensional Effects," Graduate Aeronautical Laboratories Report, Report No. SM 84-2, March, 1984.

11. Shih, C. F. and German, M. D., "Requirements for a One Parameter Characterization of Crack Tip Fields by the HRR Singularity," *International Journal of Fracture*, Vol. 17, 1981, p. 27.

12. Beinert, J., Kalthoff, J.F., "Experimental Determination of Dynamic Stress Intensity Factors by Shadow Patterns," in *Mechanics of Fracture*, Vol. 5, Sih, G.C., ed., Noordhoff, Leyden, 1979.

13. Ramberg, W., Osgood, W. R., "Description of Stress-Strain Curves by Three Parameters," NACA Technical Note No. 902, 1943.

FIGURE CAPTIONS

Figure 1: Schematic diagram of the formation of the caustic envelope obtained by reflection from [1].

Figure 2: Numerical prediction of the initial curve shape for n = 2, 3, 5, 9, 25.

Figure 3: Simulated reflected optical field for a rectangular array of light incident on the crack tip region. Caustic curve for n = 1 and n = 3 from [1].

Figure 4: Numerical prediction of the caustic curve shape for n = 2, 3, 5, 7, 9, 13, 25, 100 [from equation (2.4)].

Figure 5: Various stress and strain fields at the crack tip.

Figure 6: Definition of dimensions referred to plastic zone and initial curve.

Figure 7: Variation of the functions $R_o(n)$, $R_i(n)$, $R_c(n)$ with the strain hardening exponent n.

Figure 8: Test arrangement showing modified DCB specimen and instrumentation for load-displacement/caustics study.

Figure 9: Optical set-up for static caustics study.

Figure 10: Quasi-static tensile curves for materials tested.

Figure 11: Experimental record of the load per unit thickness versus displacement for a/W = 0.66. Average curve of three specimens tested.

Figure 12: Reference values J(P,δ) as a function of δ, calculated from equation (3.1).

Figure 13: Experimental caustic envelope (D, z_o) corresponding to one value of the load P applied to specimen number 3. Specimen with a blunt crack tip and a thickness B = 12.7 mm.

Figure 14: Ratio of J_s evaluated from shadow spot measurements divided by the reference value J(P,δ) versus the distance r_o from the crack tip divided by the thickness B for one value of J(P,δ) at the crack tip of the specimen number 3.

Figure 15: Experimental caustic envelopes (D, z_o) for three values of the load P. Specimen number 4 with a sharp crack tip and a thickness B = 6.30 mm.

Figure 16: Variation of J_s evaluated from shadow spot measurements versus the distance r_o from the crack tip divided by the thickness B, for three different values of J(P,δ) at the crack tip of the specimen number 4.

Figure 17: Photographs of caustics obtained with the tool steel, specimen number 4. The photographs are taken at one load but for two different distances z_o and hence two different sizes of the initial curve, as specified by r_o/B.

Figure 18: Experimental records of load per unit thickness versus displacement for two values of the ratio a/W tested.

Figure 19: Reference values $J(P,\delta)$ as a function of δ, calculated from equation (3.1).

Figure 20: Experimental caustic envelopes (D, z_o) for different values of the load P applied to specimen number 1. Specimen with a blunt crack tip and a thickness B = 11.43 mm.

Figure 21: Ratio $J_s/J(P,\delta)$ versus r_o/B for different reference values $J(P,\delta)$ at the crack tip of specimen number 1.

Figure 22: Experimental caustic envelopes (D, z_o) for different values of the load P applied to the specimen number 2 with a blunt crack tip and a thickness B = 6.48 mm.

Figure 23: Ratio $J_s/J(P,\delta)$ versus r_o/B for different reference values $J(P,\delta)$ at the crack tip of the specimen number 2.

Figure 24: Photograph of a caustic obtained with the 304 stainless steel, specimen number 2. The photograph is taken at one load, and for one distance z_o such that the initial curve is located inside the HRR dominated region.

Table 1. Chemical Compositions of the Two Steels (weight %)

	C	Mn	Si	Cr	W	V	P	S	Ni
Tool Steel	0.90	1.12	0.30	0.50	0.50	0.15			
304 Stainless Steel	0.08	2.00	1.00	19.00			0.045	0.030	10.00

Table 2. Comparison of Initial Curve Radius with Plastic Zone Size R_p and Specimen Thickness B, for the Tool Steel (n = 4.26)

Blunt Crack Tip (0.5 mm wide)

Specimen No. 3 B = 12.7 mm b = W - a = 94.5 mm

J(P,δ) (MPa mm)	r_o/B		r_{ox}/R_{px}		r_{oy}/R_{py}	
	Minimum Value	Maximum Value	Minimum Value	Maximum Value	Minimum Value	Maximum Value
87.71	0.493	0.560	0.312	0.355	0.332	0.378
98.82	0.490	0.641	0.300	0.391	0.330	0.432
109.47	0.550	0.650	0.321	0.379	0.344	0.406

Sharp Crack Tip (0.27 mm wide)

Specimen No. 4 B = 6.3 mm b = W - a = 95 mm

J(P,δ) (MPa mm)	r_o/B		r_{ox}/R_{px}		r_{oy}/R_{py}	
	Minimum Value	Maximum Value	Minimum Value	Maximum Value	Minimum Value	Maximum Value
25.8	0.508	0.604	0.206	0.245	0.215	0.256
40.14	0.564	0.724	0.172	0.221	0.171	0.219
47.7	0.594	0.786	0.172	0.228	0.180	0.238

Table 3. Comparison of Initial Curve Radius with Specimen Thickness B, for 304 Stainless Steel (n = 5.90). Both Specimens Have a Blunt Crack Tip (0.5 mm wide)

Specimen No. 1 B = 11.43 mm b = W - a = 94.87 mm

J(P,δ) (MPa mm)		12.42	17.61	29.72	71.96
r_o/B	Minimum Value	0.482	0.470	0.518	0.532
	Maximum Value	--	0.612	0.633	0.675

Specimen No. 2 B = 6.48 mm b = W - a = 85 mm

J(P,δ) (MPa mm)		3. 92	7. 07	13. 23	20. 75	27. 87	36. 73
r_o/B	Minimum Value	0.568	0.585	0.590	0.633	0.590	0.610
	Maximum Value	0.654	0.680	0.676	0.735	0.680	0.668

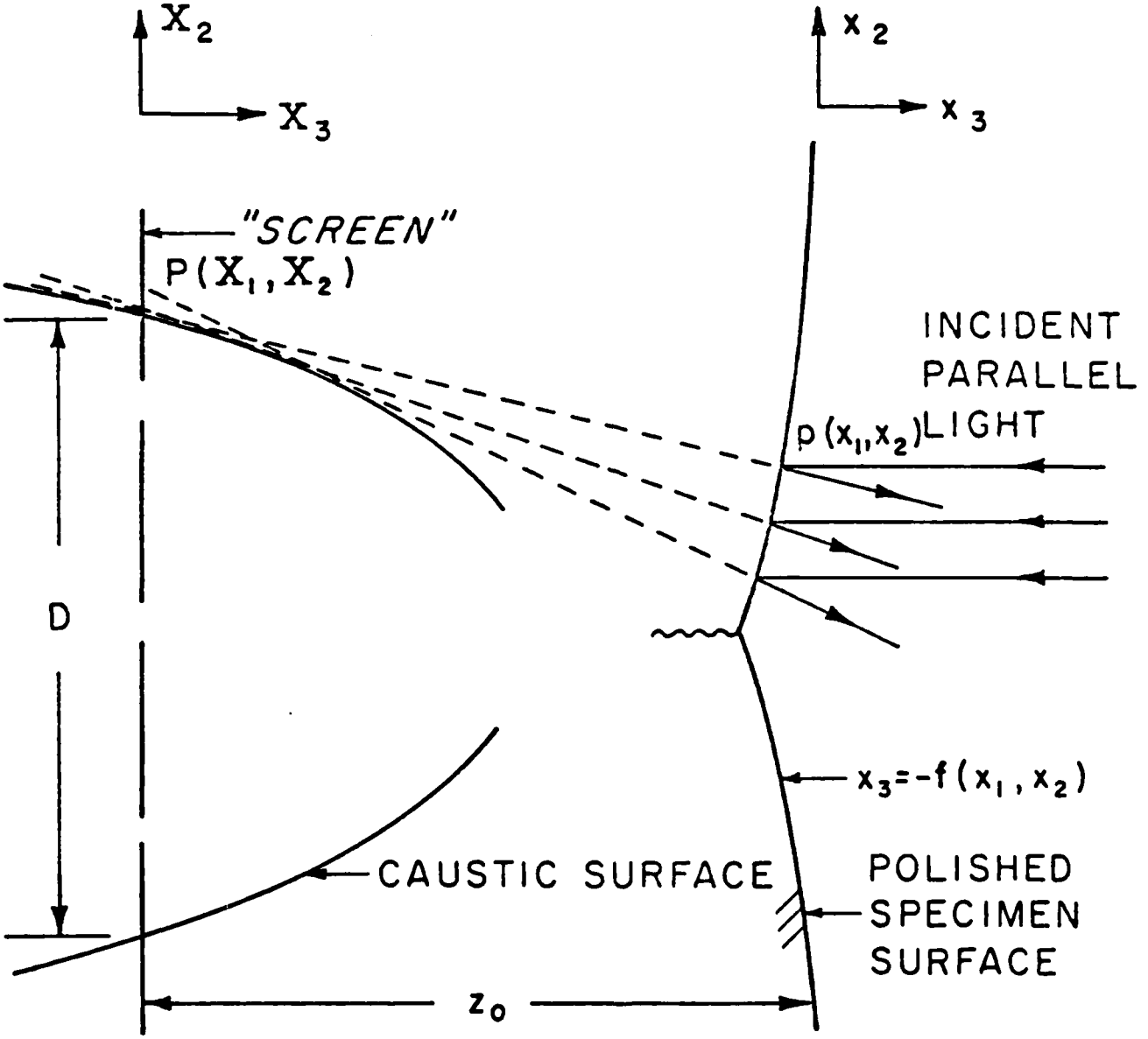
X2
X3
x2
x3
"SCREEN"
P(X1, X2)
INCIDENT
PARALLEL
p(x1,x2)LIGHT
D
x3=-f(x1, x2)
CAUSTIC SURFACE
POLISHED
SPECIMEN
SURFACE
z0

Figure 1

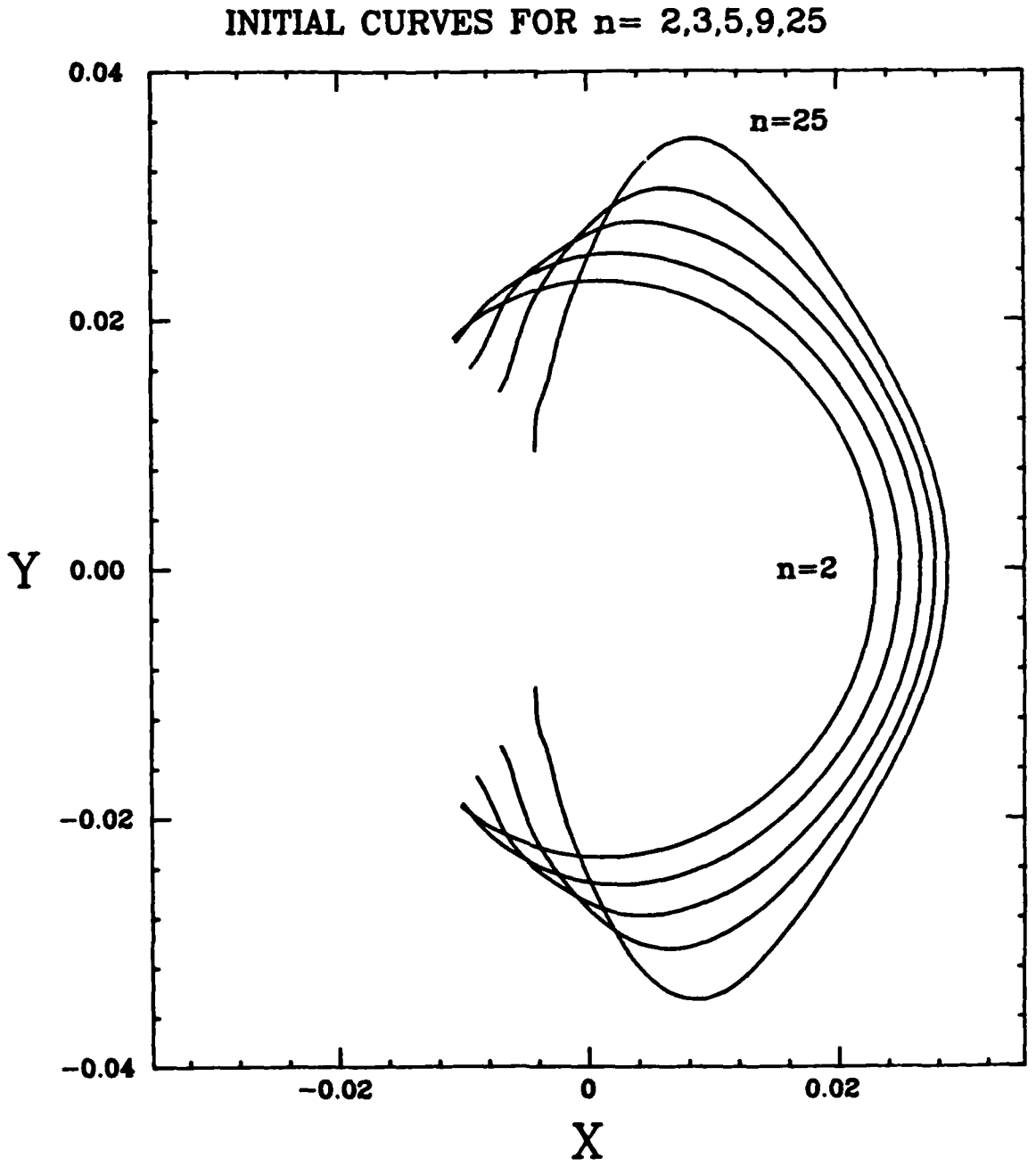
INITIAL CURVES FOR n= 2,3,5,9,25
0.04
0.02
0.00
-0.02
-0.04
Y
-0.02
0
0.02
X
n=25
n=2

Figure 2

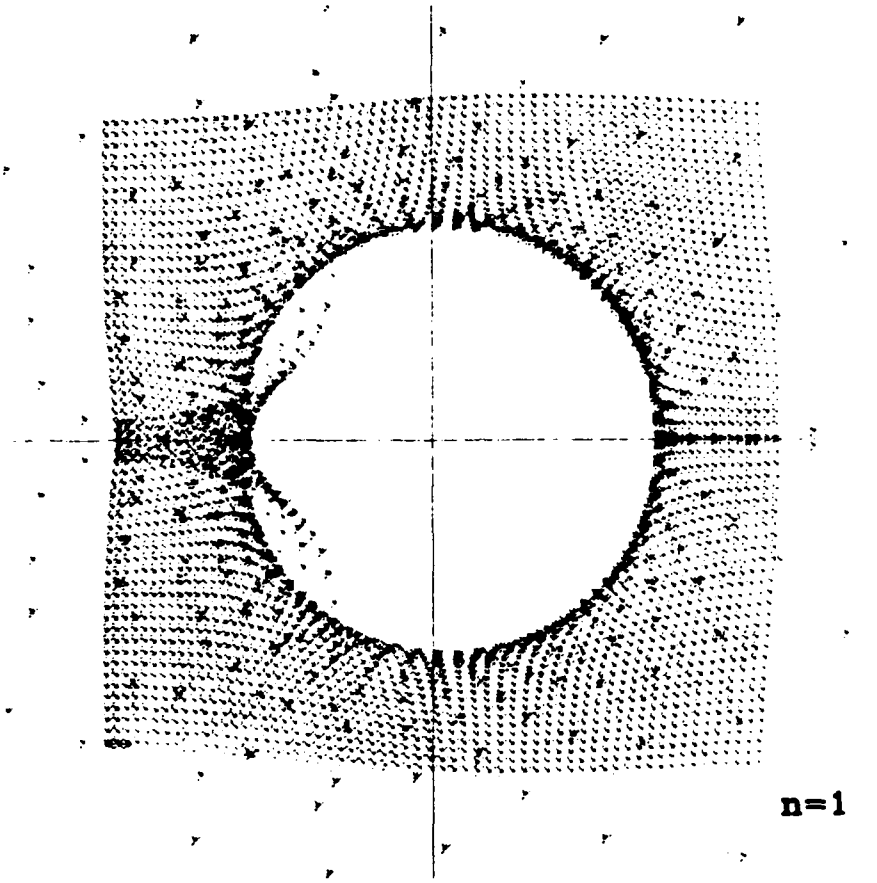

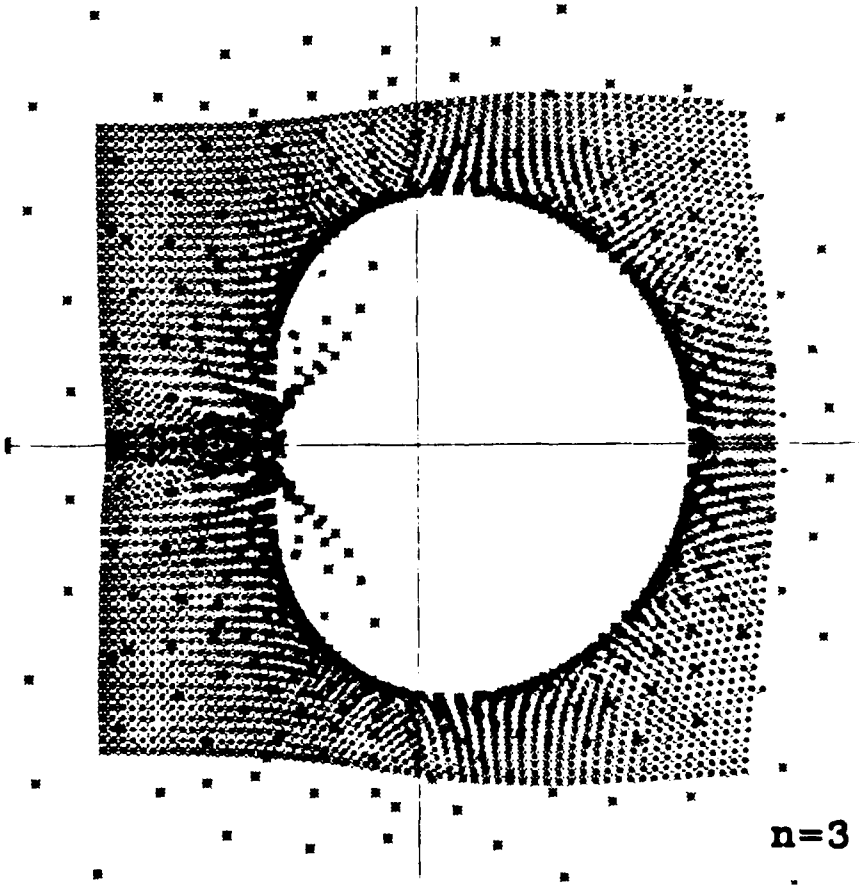

Figure 3

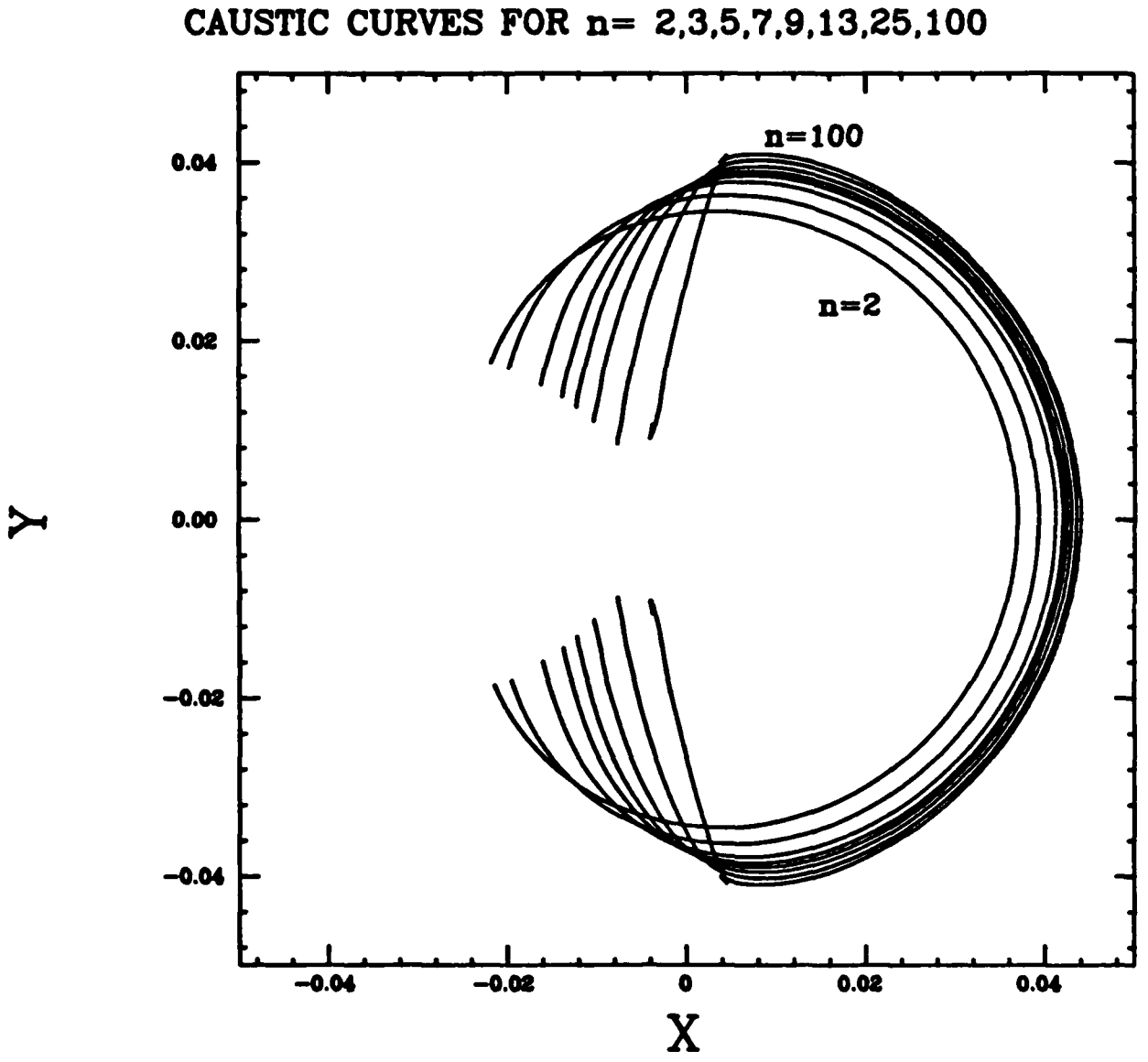
CAUSTIC CURVES FOR n= 2,3,5,7,9,13,25,100
n=100
n=2
0.04
0.02
0.00
-0.02
-0.04
Y
-0.04
-0.02
0
0.02
0.04
X

Figure 4

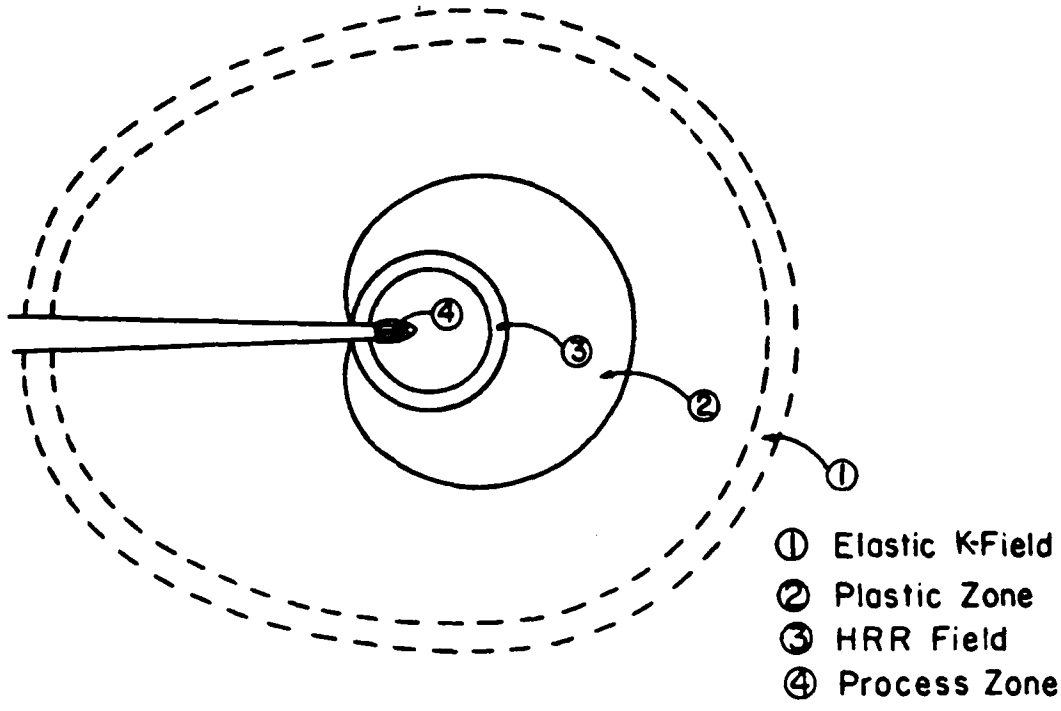

Figure 5

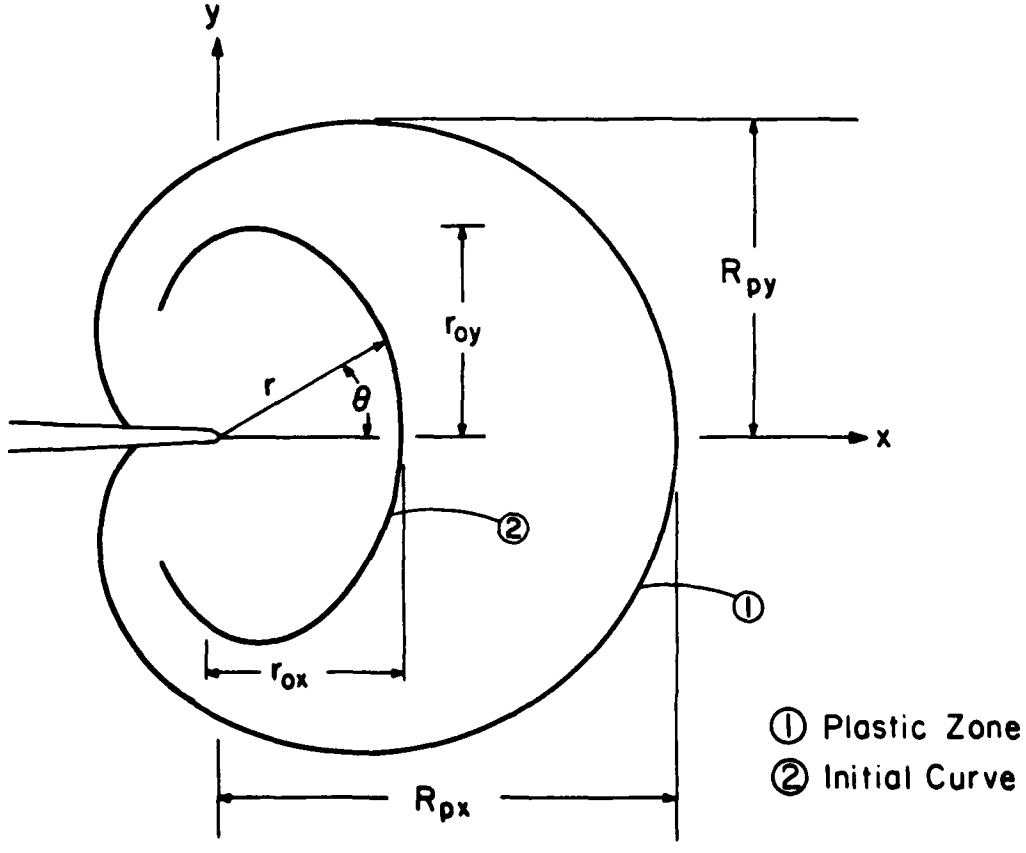

Figure 6

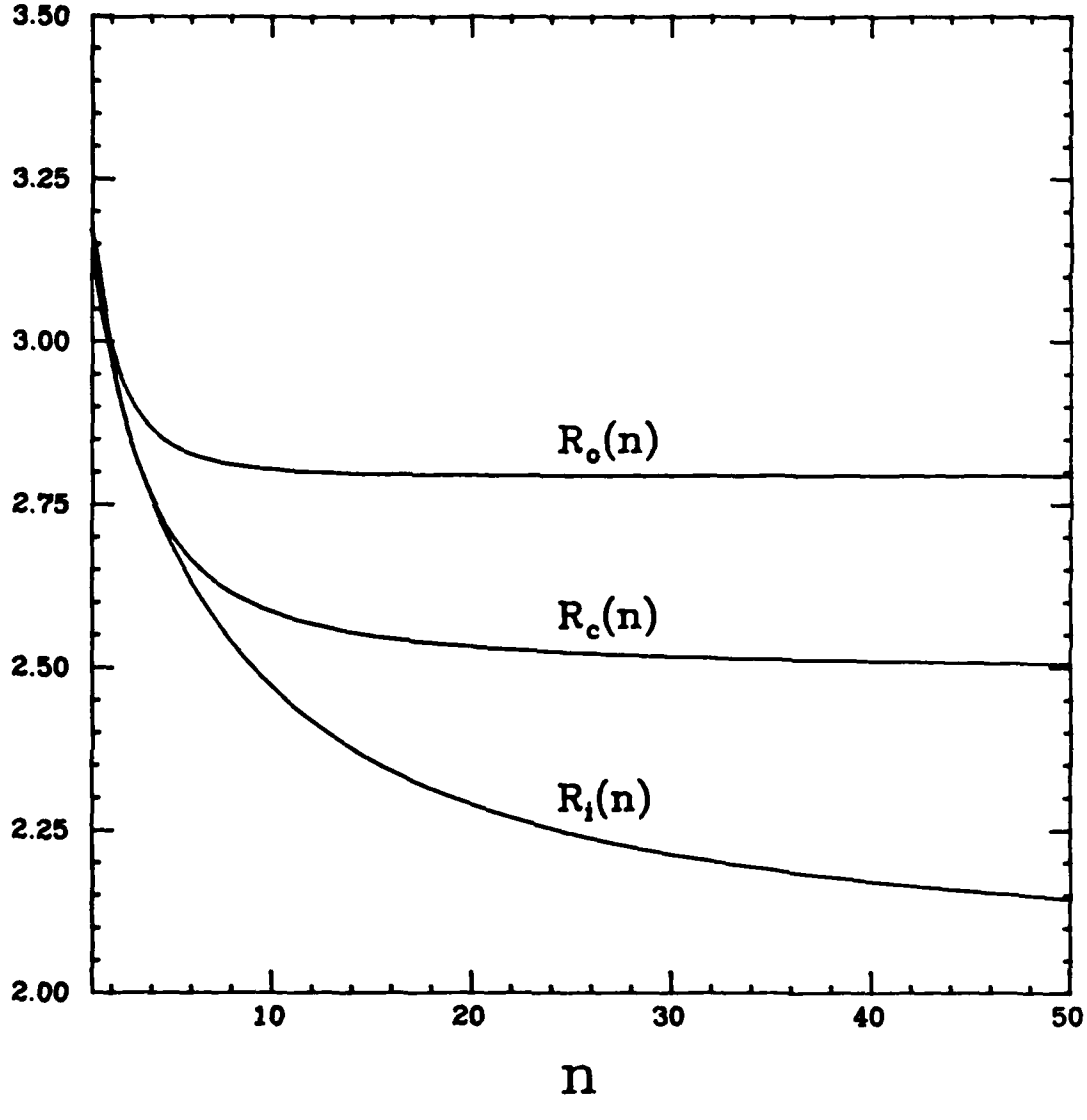

Figure 7

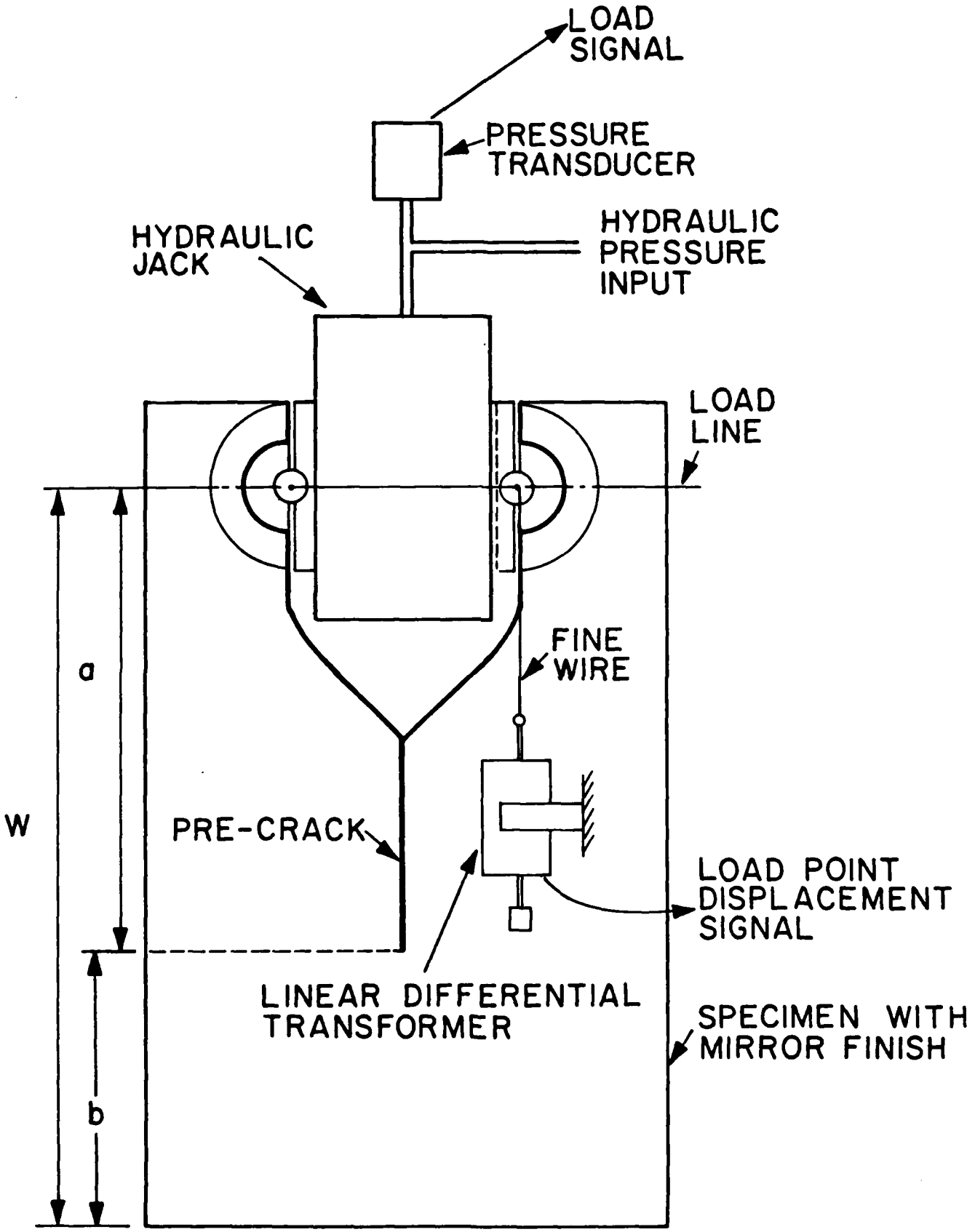
LOAD
SIGNAL
PRESSURE
TRANSDUCER
HYDRAULIC
JACK
HYDRAULIC
PRESSURE
INPUT
LOAD
LINE
FINE
WIRE
a
W
PRE-CRACK
LOAD POINT
DISPLACEMENT
SIGNAL
LINEAR DIFFERENTIAL
TRANSFORMER
SPECIMEN WITH
MIRROR FINISH
b

Figure 8

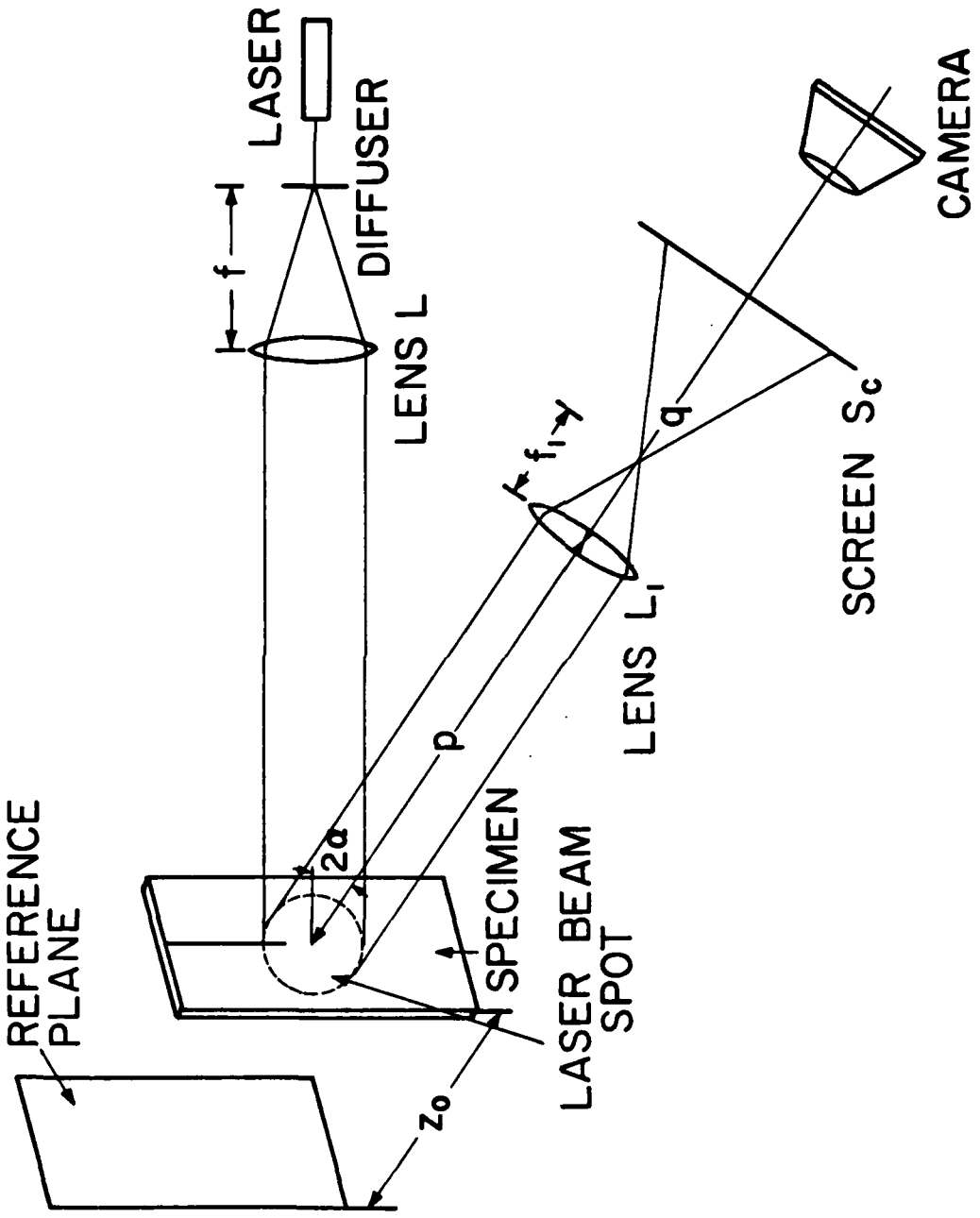
LASER
DIFFUSER
f
LENS L
f_1
q
CAMERA
SCREEN S_c
p
LENS L_1
2α
SPECIMEN
LASER BEAM SPOT
REFERENCE PLANE
z_o

Figure 9

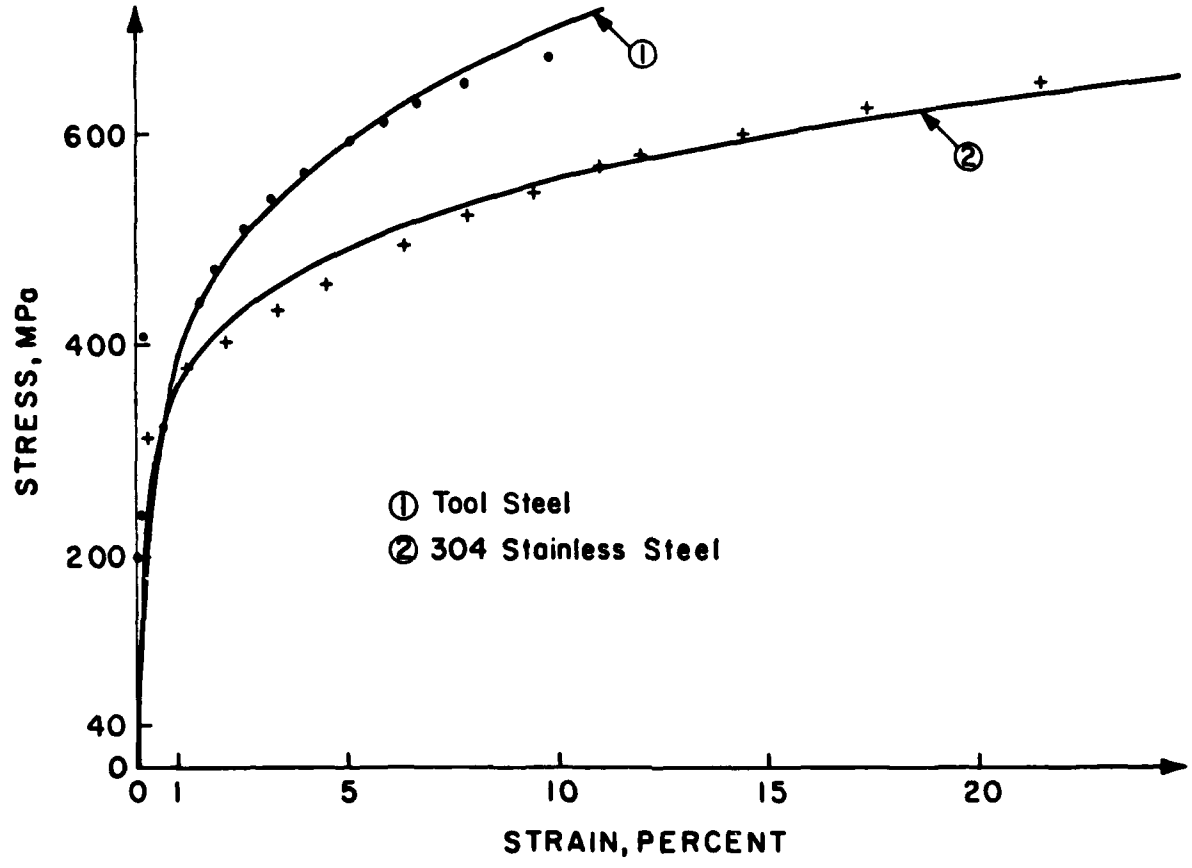

Figure 10: Points represent experimental values. The solid lines are computed stress-strain curves with the following parameters:

Material	Yield Stress σ_0 (MPa) at $\epsilon_0 = 0.002$	Parameters in Ramberg-Osgood Law, Equation (3.8)		
		Range of Applicability	Hardening Exponent n	Coefficient α
Tool Steel	408	$0.012<\epsilon<0.12$	4.26	4.82
304 Stainless Steel	323	$0.007<\epsilon<0.215$	5.90	2.069

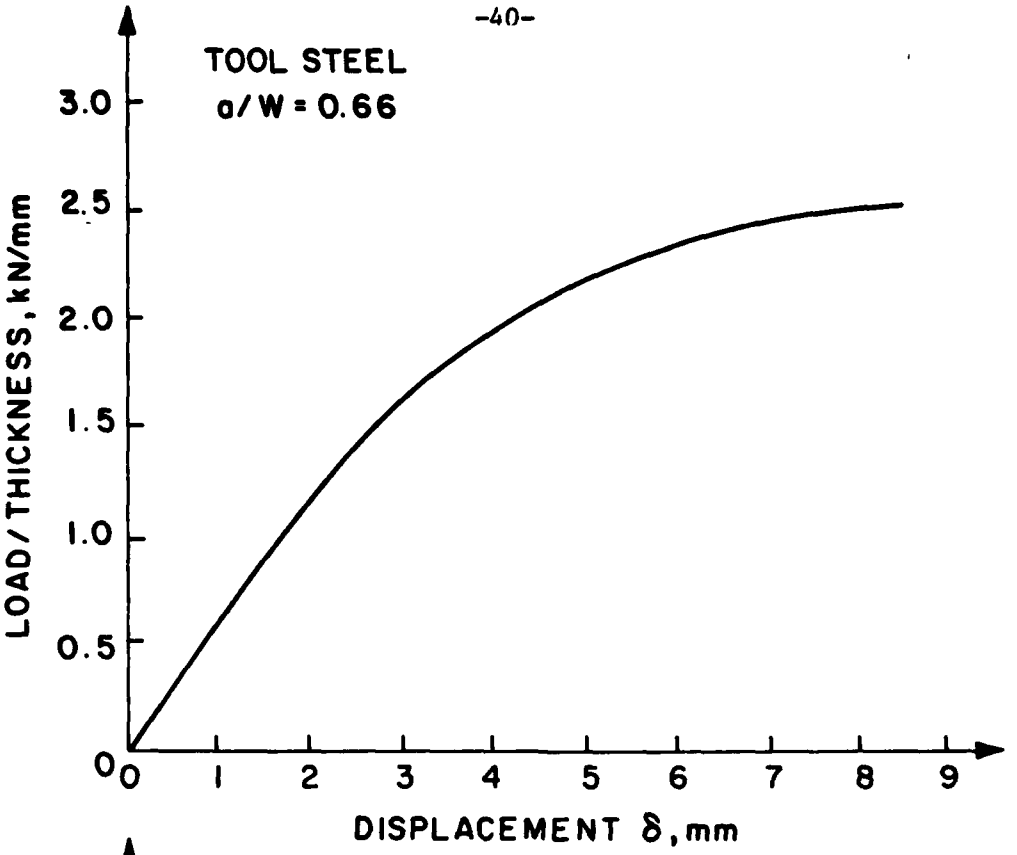

Figure 11

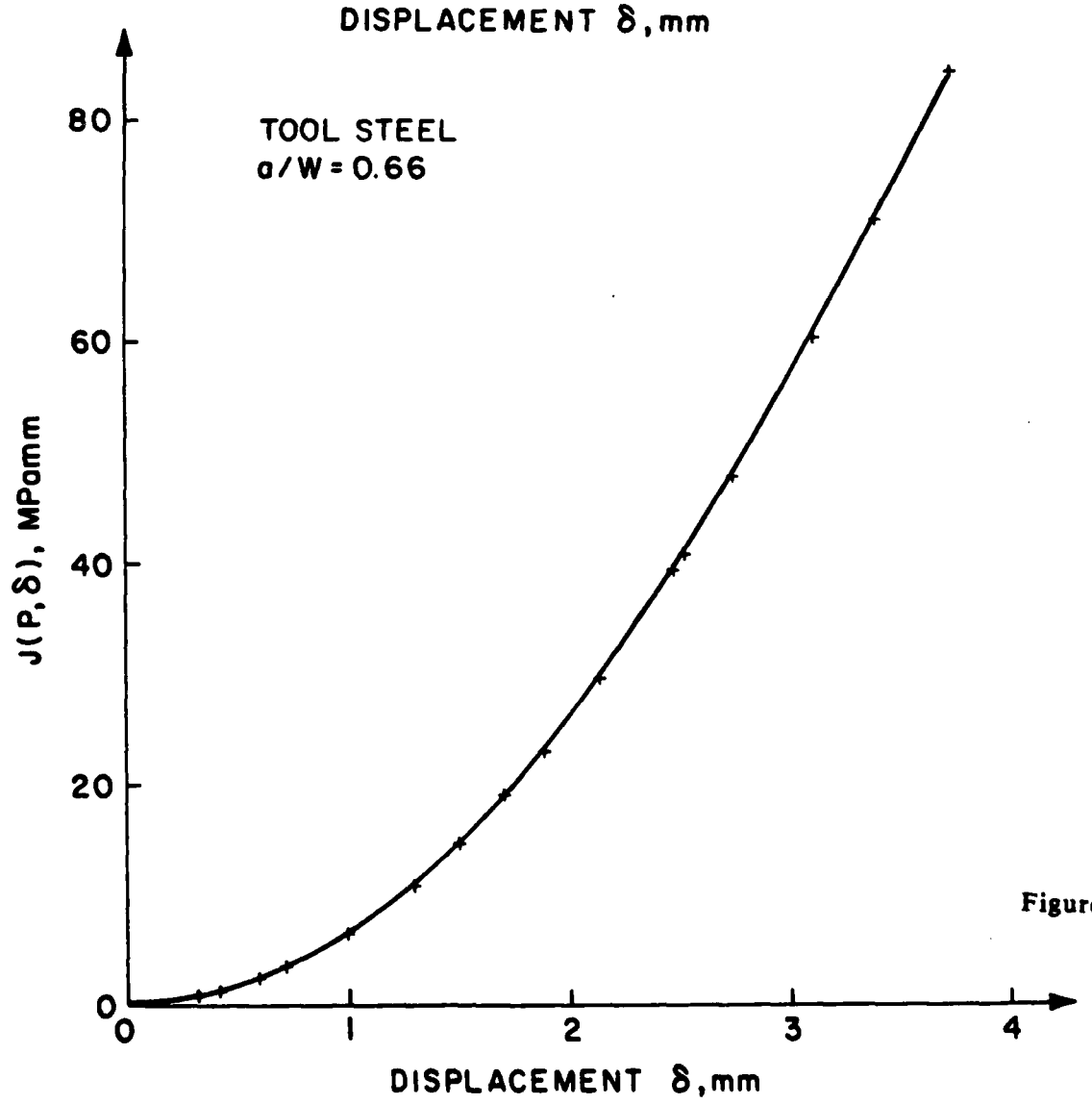

Figure 12

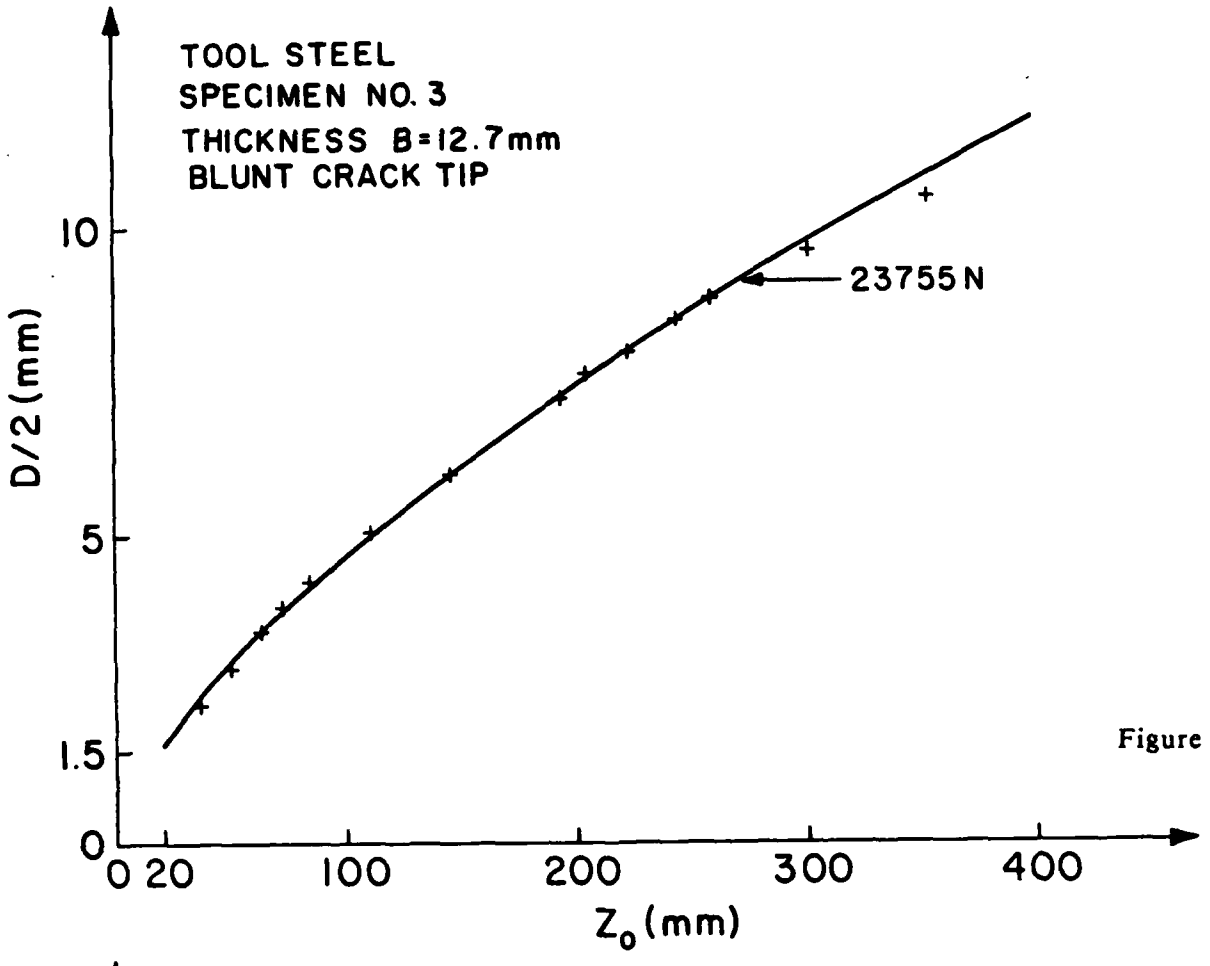

Figure 13

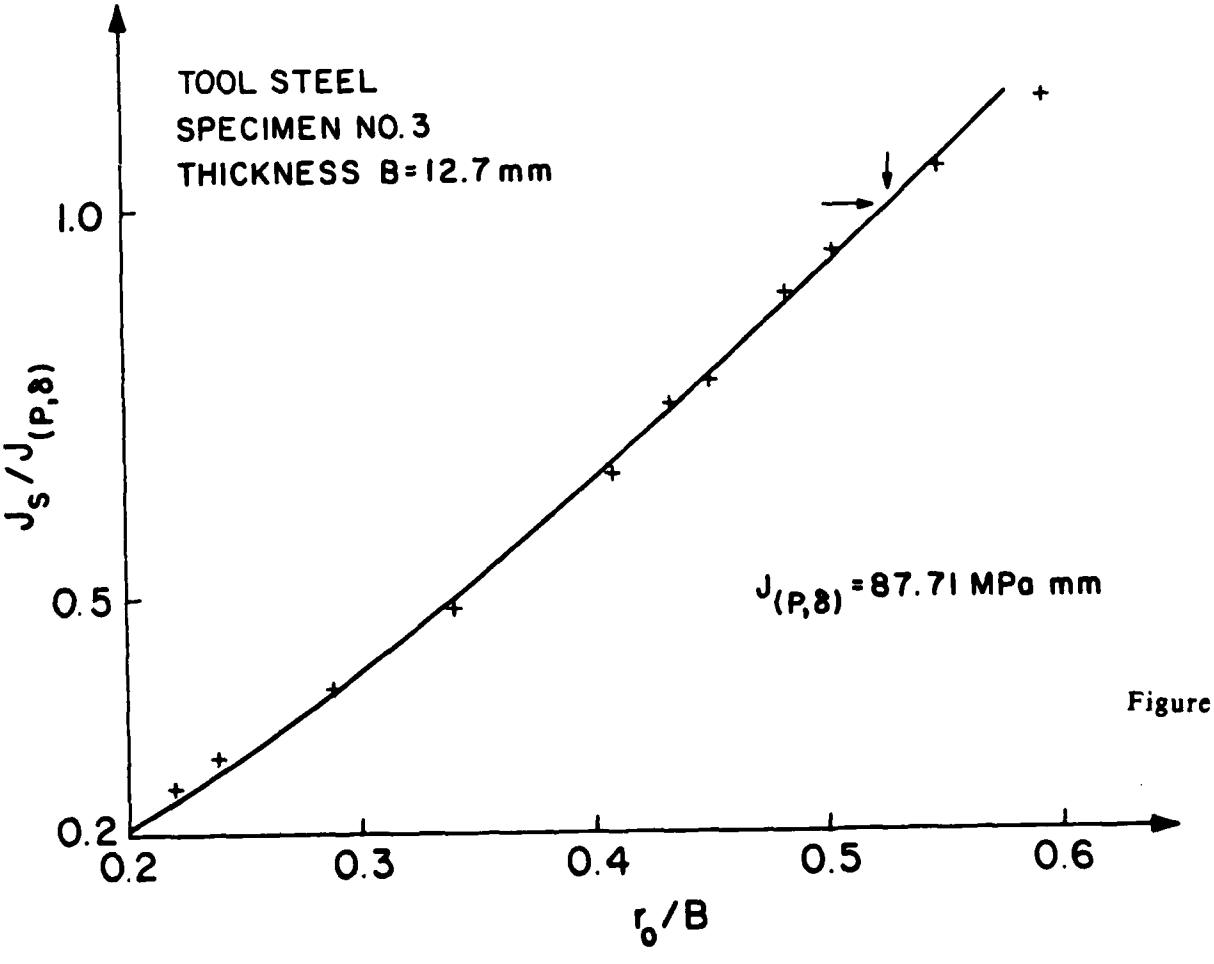

Figure 14

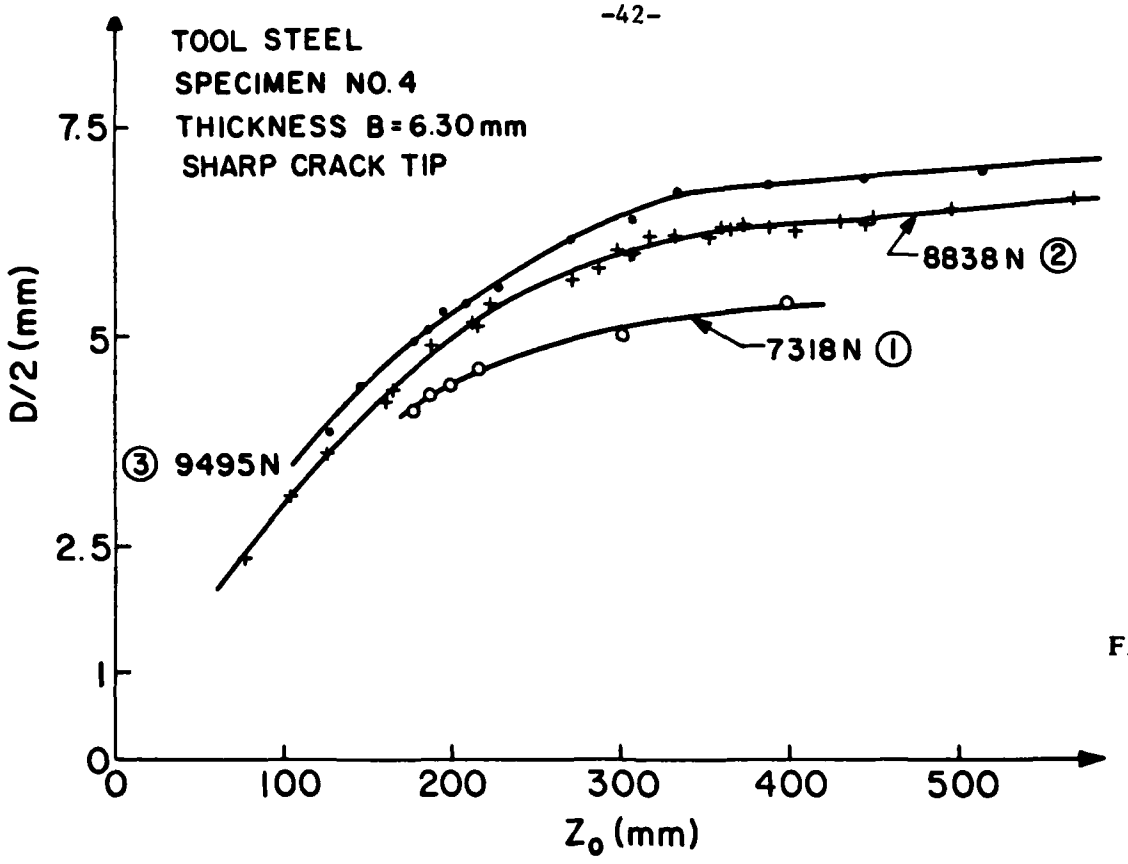

Figure 15

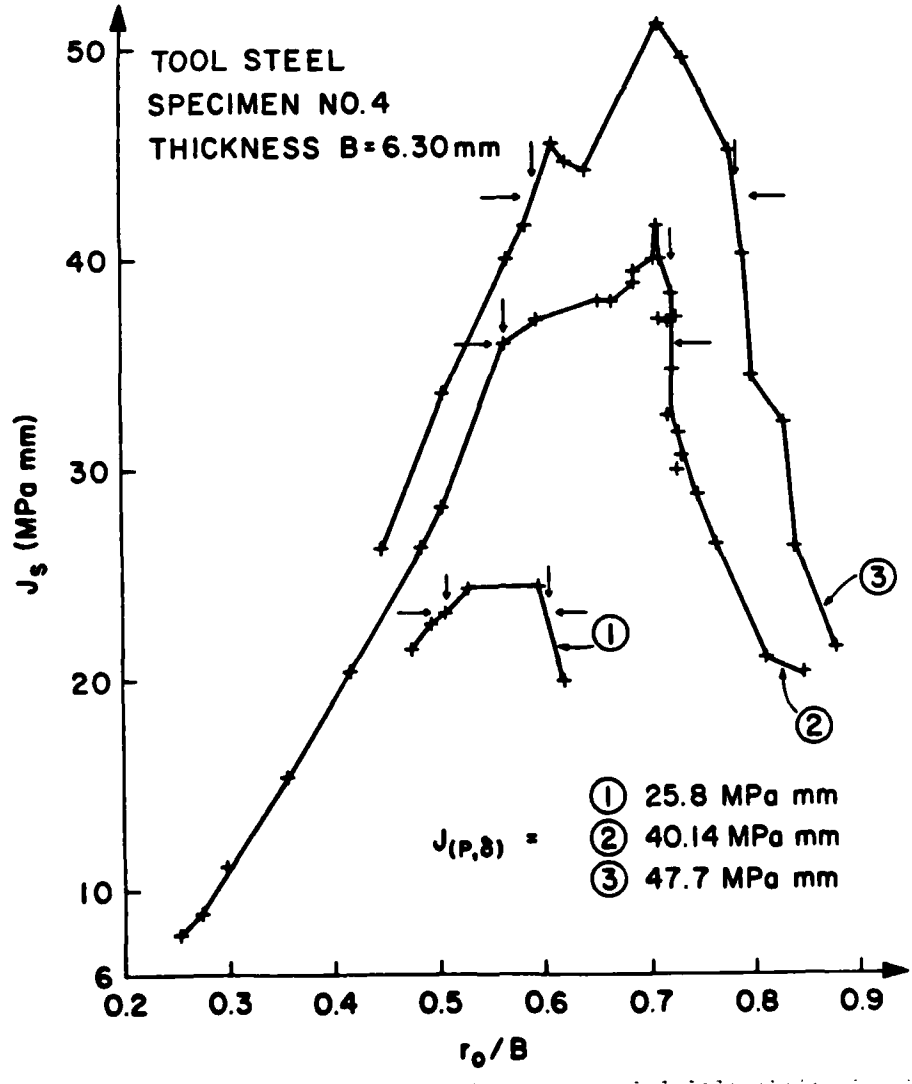

Figure 16

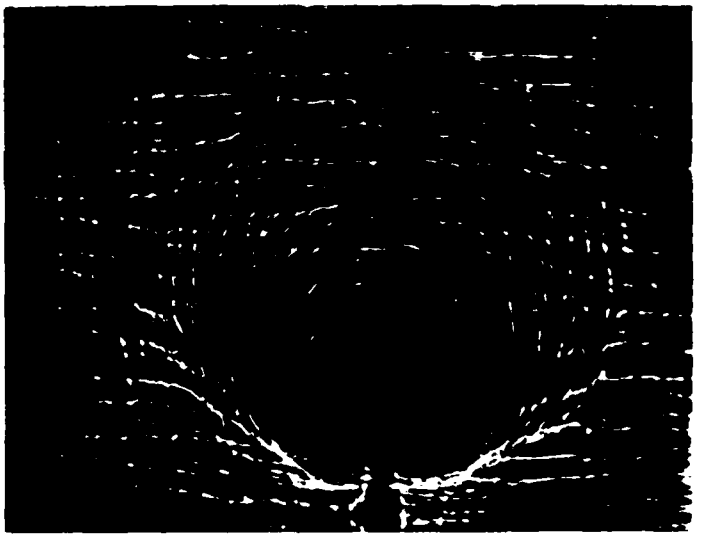

Figure 17a

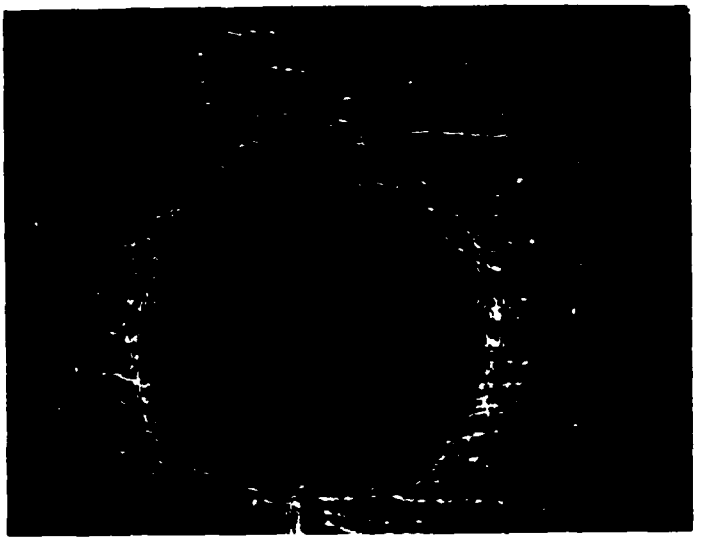

Figure 17b

	z_o mm	Magnification λ	Caustic Diameter D mm	r_o/B	$J_s/J(P,6)$	r_{cx}/r_{px}
Figure 17a	75.1	6.16	4.73	0.272	0.22	0.082
Figure 17b	200.5	4.53	9.28	0.533	1.06	0.215

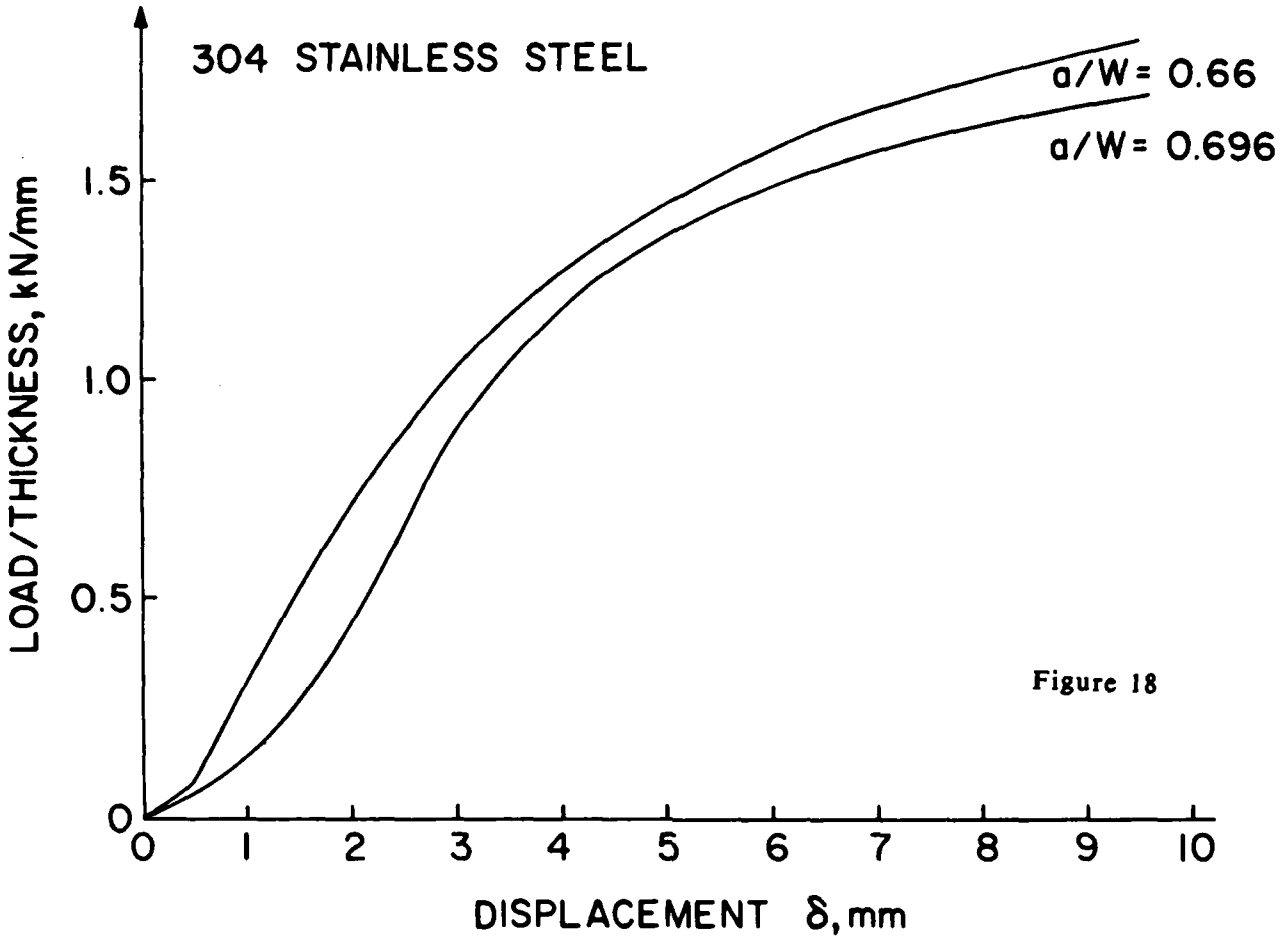

Figure 18

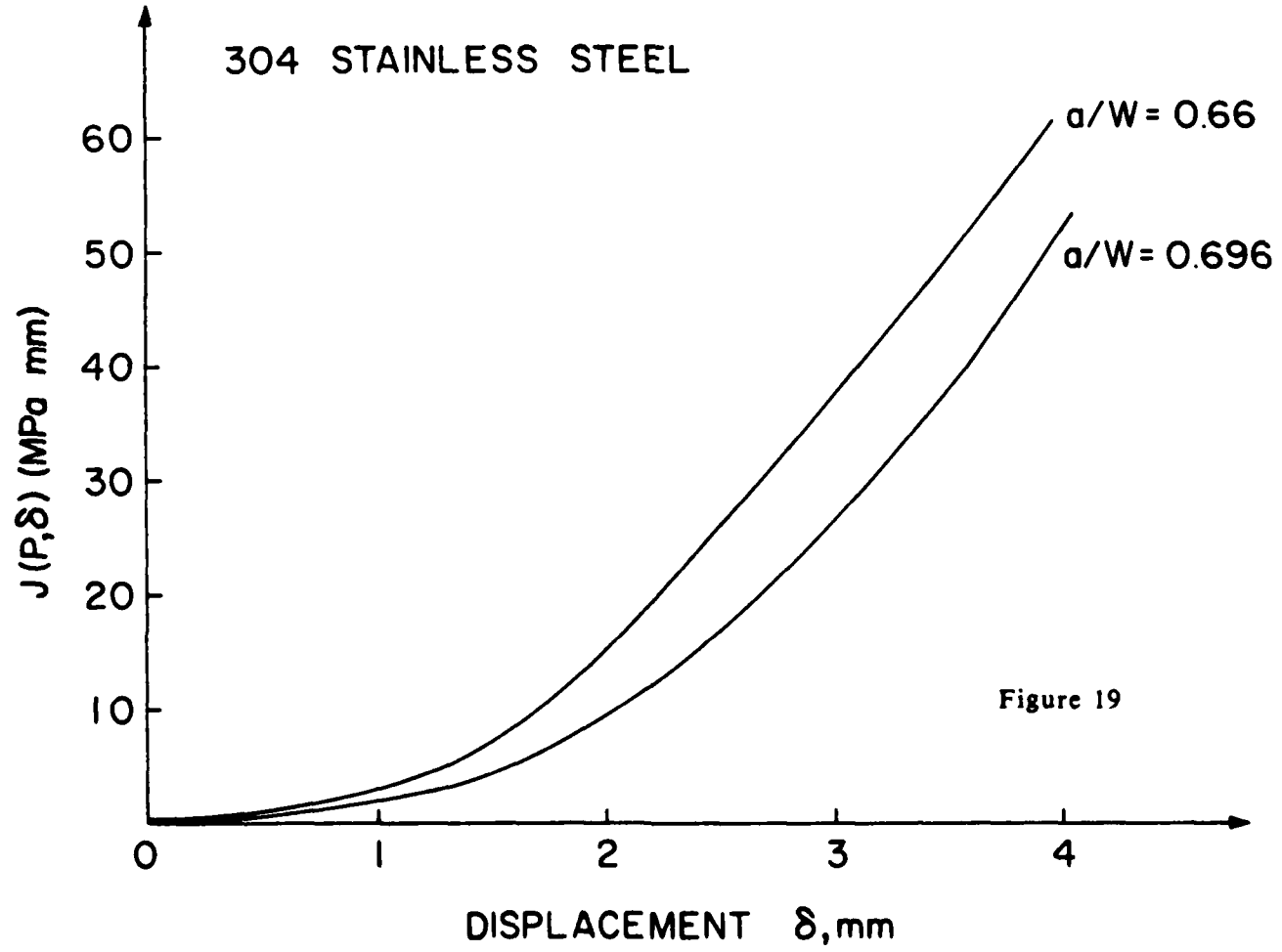

Figure 19

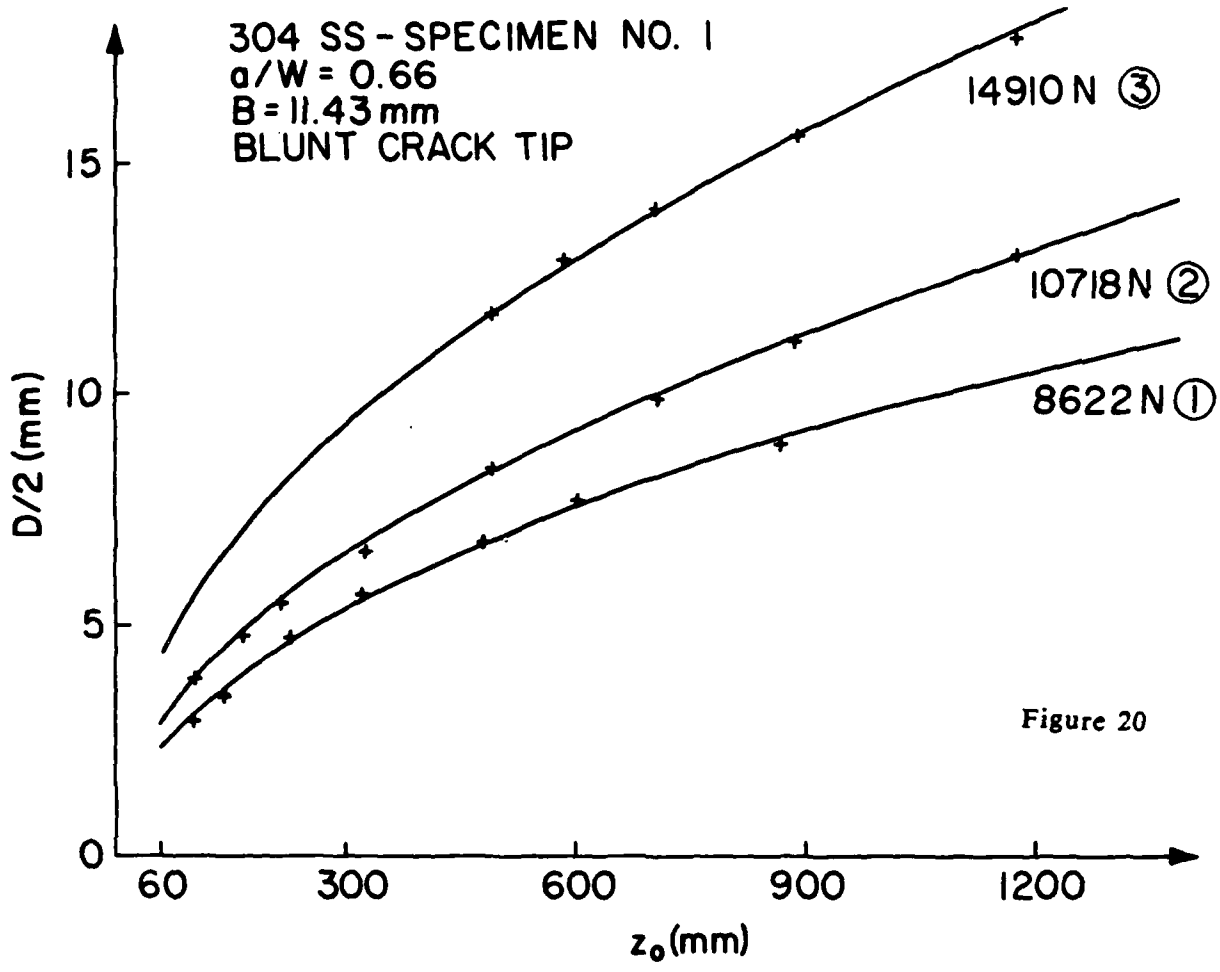

Figure 20

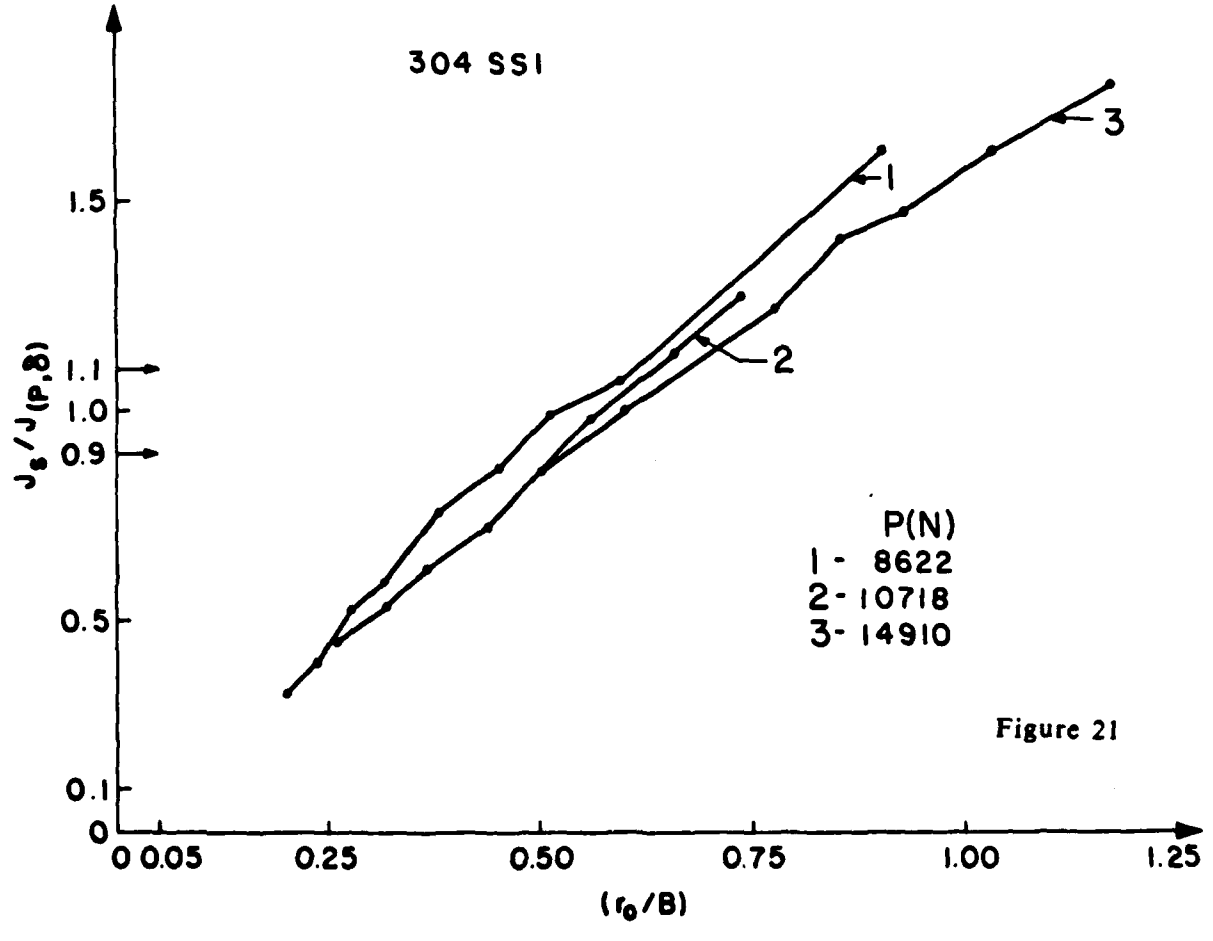

Figure 21

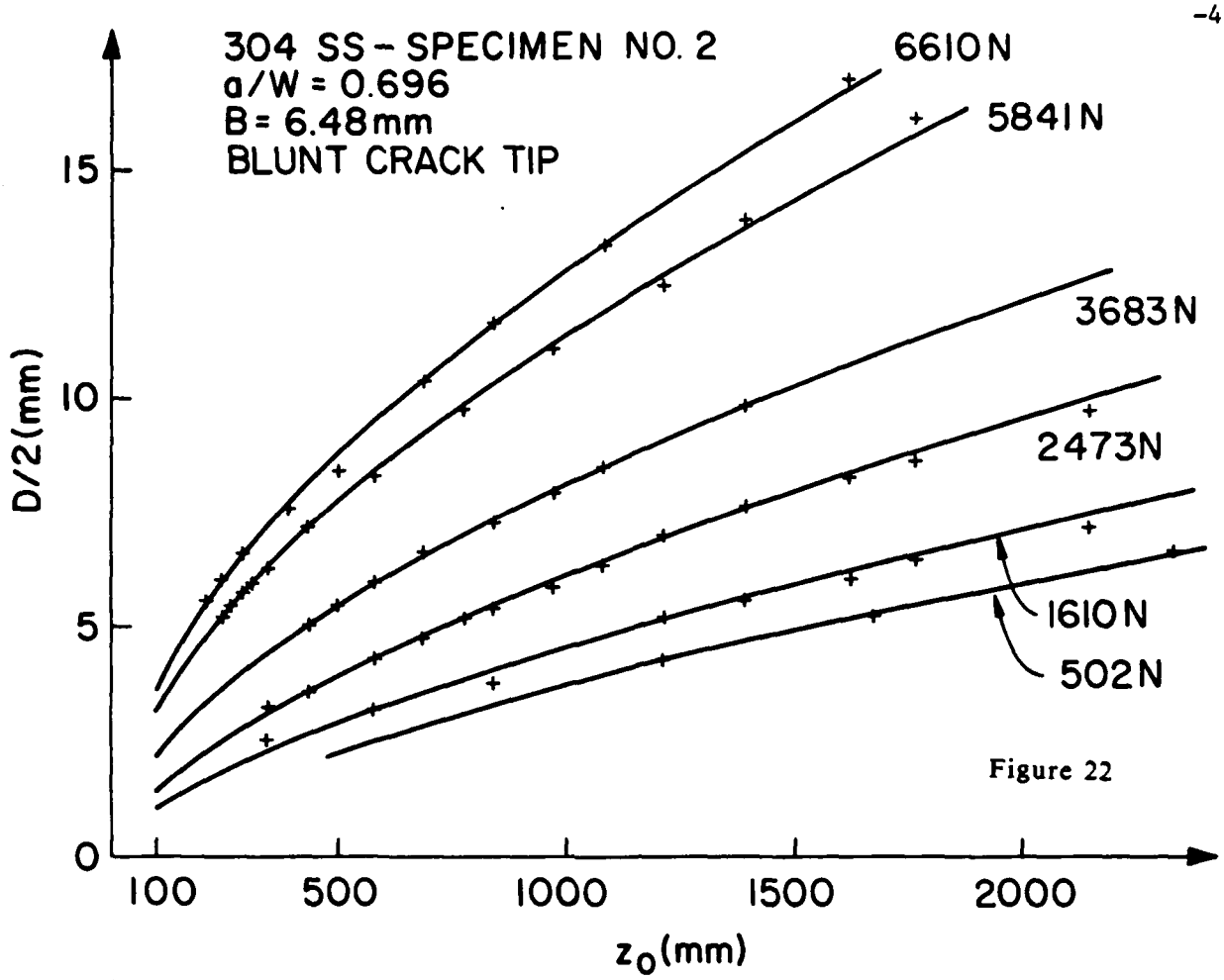

Figure 22

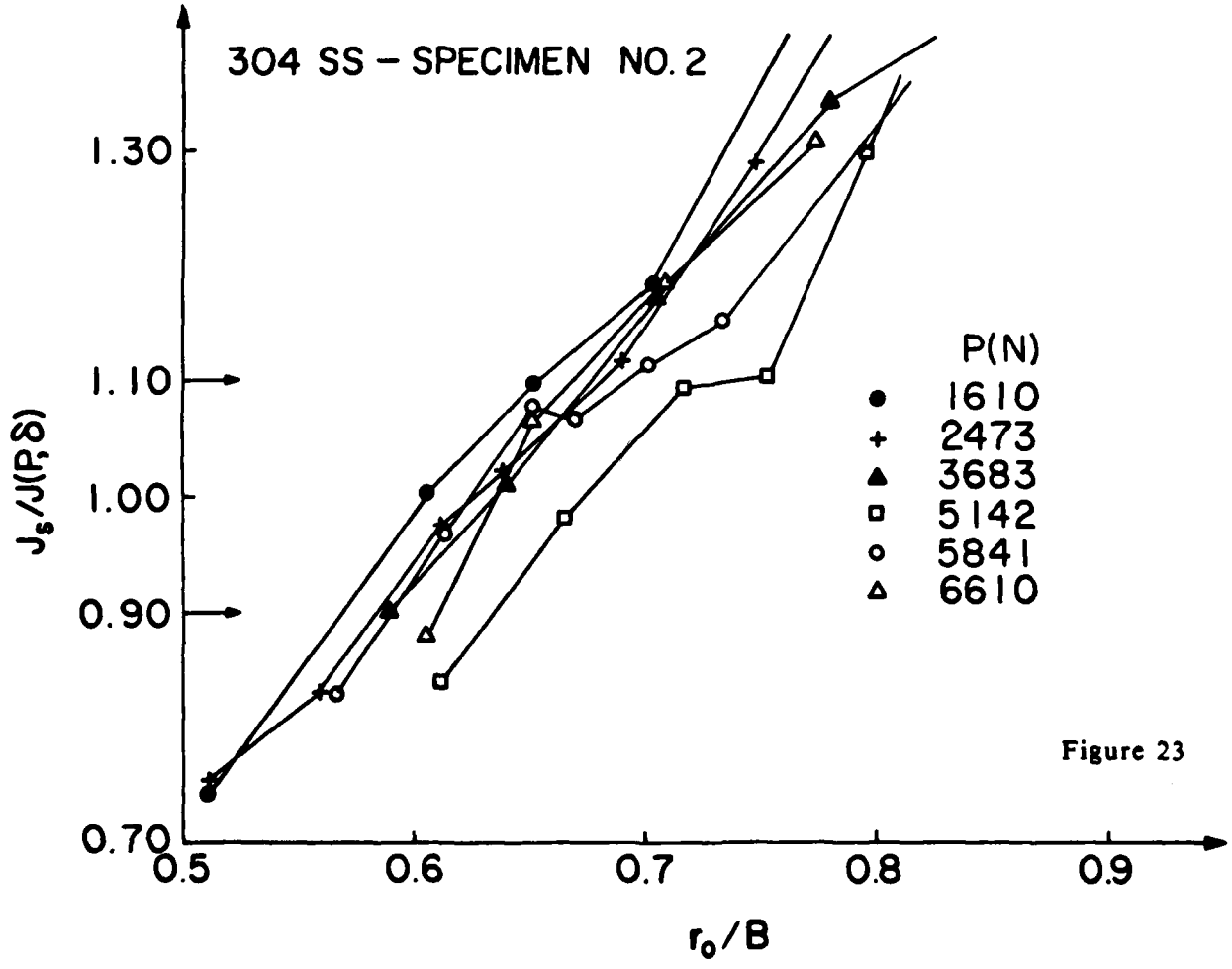

Figure 23

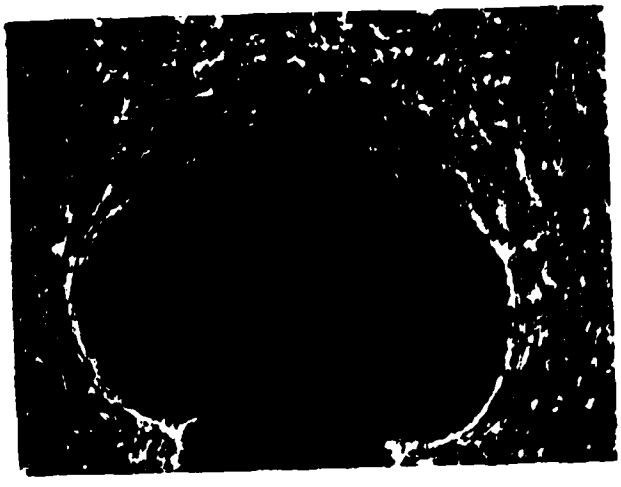

z_o mm	Magnification λ	Caustic Diameter D mm	r_o/B	$J_s/J(P,6)$
388	5.15	11.36	0.665	0.98

Figure 24

END

FILMED

5-86

DTIC